



Horizon 2020  
Programme

**GENIORS**

*Research and Innovation Action (RIA)*

This project has received funding from the European Union's Horizon 2020 research and innovation programme under grant agreement No 755171.

Start date : 2017-06-01 Duration : 48 Months  
<http://geniors.eu/>

**GENIORS**

---

**WPASR 6**

---

Authors : Mr. Stéphane BOURG (CEA), Stéphane Bourg (CEA)

GENIORS - Contract Number: 755171

Project officer: Roger Garbil

Document title	WPASR 6
Author(s)	Mr. Stéphane BOURG, Stéphane Bourg (CEA)
Number of pages	48
Document type	Deliverable
Work Package	WP11
Document number	D11.6
Issued by	CEA
Date of completion	2021-05-31 11:43:26
Dissemination level	Public

---

## Summary

Workpackage activity summary report n°6

---

## Approval

Date	By
2021-05-31 11:43:39	Mr. Stéphane BOURG (CEA)
2021-05-31 11:43:48	Mr. Stéphane BOURG (CEA)
2021-05-31 11:43:59	Mr. Stéphane BOURG (CEA)

**CONTENT**

Content.....	1
WP1 .....	5
Introduction .....	5
Main Results .....	5
Task 1.1 .....	5
Task 1.2 .....	6
Conclusions .....	6
WP2 .....	7
Introduction .....	7
Main Results .....	7
Task 2.1 Radiolysis & degradation products (TASK LEADER: Julich) .....	7
Manpower .....	7
Main Progresses .....	7
Difficulties .....	8
Action plan .....	9
Task 2.2 Destruction of organic (task leader: CEA) .....	9
Task 2.3 Gas generation (task leader: POLIMI) .....	9
Task 2.4 Radiolysis modelling (task leader: CTU) .....	10
List of publications .....	11
Conclusions .....	12
WP3 .....	13
Introduction .....	13
MANPOWER.....	13
MAIN RESULTS .....	13
TASK 3.1 OPTIMISATION OF SYSTEMS (TASK LEADER: POLIMI) .....	13
TASK 3.2 DISTRIBUTION DATA AND CHEMICAL MODELLING (TASK LEADER: KIT) .....	14

TASK 3.3 PHYSICO-CHEMICAL & LOADING (TASK LEADER: CIEMAT) .....	14
TASK 3.4 SOLVENT CLEAN-UP & RECYCLE (TASK LEADER:>NNL.....	15
CONCLUSIONS .....	15
wp4.....	16
Introduction .....	16
Main Results .....	16
Task 4.1 Study of the solid/liquid interfaces during dissolution [1-48] Task Leader : CNRS .....	16
List of publications.....	18
Task 4.2 Study of the solid/liquid interface during CONVERSION [1-48] Task Leader : SCK.CEN.....	19
List of publications .....	21
Conclusions.....	21
wp5.....	22
Task 5.1 .....	22
Manpower.....	22
Main Progresses .....	22
Action plan .....	22
Task 5.3 .....	23
Manpower.....	23
Main Progresses .....	23
Difficulties .....	23
Action plan .....	23
List of publications .....	23
wp6.....	24
Introduction .....	24
Main Results .....	24
Task 6.1: Homogeneous recycling.....	24

6.2 HETEROGENEOUS RECYCLING.....	34
Conclusions .....	34
WP7 .....	35
Introduction .....	35
Main Results .....	35
Task 7.1 .....	35
Task 7.2 .....	35
Task 7.3 .....	36
Task 7.4 Characterizations .....	36
Conclusion.....	36
WP8 .....	37
Introduction .....	37
Main Results .....	37
Task 8.1 to 8.3 .....	37
Task 8.4 .....	37
Main Progresses .....	37
Task 8.5 .....	38
Conclusions.....	38
wp9.....	39
introduction .....	39
Main Results .....	39
Task 9.2 .....	39
Manpower .....	39
Main Progresses .....	39
Task 9.3 .....	43
wp10.....	45
Main Results .....	45
Task 10.1 Clustering Events.....	45

Task 10.2 Stakeholders Events.....	45
Conclusions.....	46
wp12.....	47
Introduction.....	47
Main Results .....	47
Task 421 .....	47
Task 422 .....	47
Task 423 .....	47
Action plan .....	47

## WP1

### INTRODUCTION

WP1 aims at investigating the solution and extraction chemistry of key fission products. This research is important to improve the actinide/fission product separation and then to further optimize the separation processes. It includes extraction chemistry of problematic fission products (Task 1.1) and the optimization of scrubbing steps during co-extraction (Task 1.2).

### MAIN RESULTS

#### TASK 1.1

##### MANPOWER

After 6 semester 100 % of efforts planned for the complete were realized. Tasks 1.1 and 1.2 are now completed

##### MAIN PROGRESSES

##### Sr(II) EXTRACTION INTO TODGA

In a solvent extraction process using the commonly applied TODGA solvent (0.2 mol/L TODGA + 5 vol.% 1-octanol in TPH), Sr(II) is extracted in the extraction section ( $DSr(II) \approx 7$ ) and scrubbed in the scrubbing section ( $DSr(II) \approx 0.3$ ), see Figure 1. This leads to significant Sr(II) accumulation in the extraction section. Reducing the TODGA concentration to 0.1 mol/L would mitigate this behaviour. As with the 1-octanol/TPH diluent, accumulation of Sr(II) is expected in a process using the TODGA-DIPB diluent if the TODGA concentration is greater than 0.1 mol/L.

##### BEHAVIOUR OF Fe(III) IN TODGA SYSTEMS

The extraction of  $^{55}\text{Fe(III)}$  into TODGA was studied as iron is discussed as one of the possibly problematic fission and corrosion products in the i-SANEX7 and AMSEL8 processes. Therefore, the extraction of Fe(III) was studied as a function of nitric acid and TODGA concentrations. Figure 8 shows that low distribution ratios were observed under all conditions. Nevertheless, a slight increase in distribution ratios is observed for very low and for higher  $\text{HNO}_3$  concentrations.

##### EXTRACTION AND SPECIATION OF Ru(III)

The results have shown that none of the studied extractants interacts with ruthenium directly, after extractions from 4 mol/L nitric acid. The same analysis performed at 3 mol/L nitric acid provide identical conclusions. The absence of extractant-ruthenium interaction was proven by the absence of a carbonyl/phosphoryl and nitrosyl shifts in the FTIR spectra, and by EXAFS spectroscopy. Furthermore, all spectra indicate a similar inner sphere coordination of ruthenium in 4 mol/L nitric acid and in all corresponding organic solvents after extraction. Differences in the ruthenium distribution ratios for

extraction from 4 mol/L nitric acid are driven by outer-sphere interactions in all solvents analysed. TBP, MOEHA and TODGA predominantly bond to water ligands of ruthenium nitrosyl complexes during extraction. Such hydrogen bond-driven solvent extraction results in a linear relation between ruthenium and water extraction (Figure 10). Consequently, solvents extracting high concentrations of water should favour higher ruthenium co-extraction.

Currently there is no fully adequate explanation for the retention phenomenon of ruthenium. The difference in distribution ratio between extraction and back extraction is independent of the extraction system and hence might concern the ruthenium coordination sphere itself. Speciation study identified numerous transformations of ruthenium in solvent extraction cycles that could explain the retention phenomenon. For instance, enlarged nitrous acid concentration in the initial aqueous phase strongly changes extracted species of ruthenium and could be involved in the retention process. In this case, the change in coordination mode of the extracting molecule may be involved in this process (inner sphere vs. outer sphere coordination). The impact of hydroxide ligand in the stripping steps must be considered too since. Moreover, future studies to understand and predict the retention mechanism likely deserve kinetic experiments since ruthenium nitrosyl complexes are known slowly exchange ligands.

Overall, the ruthenium extraction and back extraction was studied for different extraction systems all showing promising properties in means of ruthenium selectivity (low DRu). Nevertheless, the retention mechanism identified already for TBP is also evidenced for the other studied extracting molecule (TODGA, MOEHA). From the speciation analysis, we described the similarity in the ruthenium extraction process for the three studied systems mostly involving a weak hydrogen bond base ruthenium-ligand interaction. Without nitrite ions and under 3–4 mol/L nitric acid conditions, the ruthenium is extracted as nitrosyl trinitrate di aquo complexes hydrogen bonded through the water ligand to the extracting molecule. Consequently, we demonstrated that, in first approximation, the ruthenium extraction properties of a given solvent are strongly related to its ability to extract water. Further experiments demonstrated that nitrite (so far neglected) is also important for this system because it strongly interacts with ruthenium complexes in both aqueous and organic phases. Nitrite ions are stabilised for several weeks in the ruthenium coordination sphere even under highly acidic conditions. This effect appears to modify the ruthenium distribution ratio and seems important for the right prediction of Ru extraction properties. Moreover, the great change in the extracting molecule coordination mode (outer to inner sphere) in presence of nitrite ligands seems important to anticipate the molecular interaction in the organic phase. This nitrite effect is one clue to explain the ruthenium retention mechanism that was evidenced in the last part of this work. But, as already mentioned, there is still no fully satisfying explanation to explain the variation observed for DRu in the stripping steps and further kinetic studies should help to solve this puzzle.

## TASK 1.2

Completed

## CONCLUSIONS

All the work planned in WP1 is now completed

## WP2

### INTRODUCTION

The general objective of WP2 is to ensure a safe long-term performance of a chemical system submitted to radiation. To understand and improve the degradation of the ligands as well as of the extraction systems is the main goal. Solvent degradation may lead to many undesirable effects, for that, the identification of losses of efficiency, the behaviour troublesome degradation products or any mal operation situation due to degradation are the key issues. Work is divided in four task: T21 Radiolysis & degradation products; T22 Destruction of organics; T23 Gas generation and T24 Radiolysis modelling.

### MAIN RESULTS

#### TASK 2.1 RADIOLYSIS & DEGRADATION PRODUCTS (TASK LEADER: JULICH)

##### MANPOWER

9.1 mp (0.9 pm CTU, 2.7 pm IIC, 2.5 pm CIEMAT and 3 pm Juelich) were reported this semester.

##### MAIN PROGRESSES

###### Dosimetric studies:

During SCK.CEN dosimetry study to evaluate the dosimeter systems and dose rates applied in its BRIGITTE and RITA gamma irradiation facilities, the use of Red Perspex dosimeters to characterise high dose rate gamma facility was also tested. In parallel to this study, SCK.CEN sent to CIEMAT Red and Amber dosimeters from Harwell Dosimetrics's to compare with the results obtained at Náyade facility, where a Fricke dosimetry is usually performed. Despite the possible experimental deviation that could be produces because of the timing management, coherent and concordant absorbed doses were provided by Red Perspex dosimeters also at CIEMAT.

###### Stability studies of BTBP and BTPPhen:

CyMe<sub>4</sub>-BTBP and CyMe<sub>4</sub>-BTPPhen have been synthesized by UREAD in ~1 g quantity for irradiation studies. (No pm reported)

During this semester, CTU and IIC have continued the studies of CyMe<sub>4</sub>-BTBP in fluorinated diluent:

- The CHALMEX systems (0.01 M CyMe<sub>4</sub>-BTBP in 70% FS-13/30% TBP; 4 M HNO<sub>3</sub>) for Am(III) and Eu(III) extraction were tested at different temperatures and their kinetics was determined. Based on the obtained results, thermodynamic parameters (change in entropy and change in enthalpy) were calculated with negative values of  $\Delta H$  and  $\Delta S$ .

- IIC has continued with the analysis and isolation of DCs from the concentrated samples of CyMe<sub>4</sub>-BTBP (GANEX solvent) irradiated at Chalmers facilities (1200 kGy), by separations of larger volume (10 mL). An improved *semi*-preparative pre-separation of the DCs using flash chromatography led to a better removal of the solvent in the initial step. The following *semi*-preparative HPLC step afforded fractions enriched by one or several degradation products. All collected fractions were analyzed by MS and <sup>1</sup>H, <sup>13</sup>C NMR methods, and a better NMR characterization of DCs was obtained. One of main component was assigned as CyMe<sub>4</sub>-BTP, apparently persisting in the sample from synthesis. Some NMR spectra for low mass degradation products could be also relatively reliably assigned to tentative structures.

### Stability studies of diglycolamides:

#### - mTDDGA:

The radiolysis of mTDDGA was further studied and has been continued as part of Juelich-SCK•CEN collaboration. Five mTDDGA degradation compounds that had been identified before were synthesized by TWENTE and used to quantify their concentrations in irradiated samples. The C<sub>ether</sub>-O<sub>ether</sub> bond breaking product was found to be the most abundant degradation product, independent of the chemical conditions during irradiation. The precipitate formed during mTDDGA irradiation was identified as protonated didecylamine.

### Studies of SO<sub>3</sub>PhBTP and SO<sub>3</sub>PhBTP stripping or masking agents:

- CIEMAT has continued with activities to analyse quantitatively the degraded aqueous phases containing AHA or SO<sub>3</sub>-Ph-BTP. Particularly, it is being set up the methodology to measure and quantify the remaining concentration of SO<sub>3</sub>-Ph-BTP after irradiation by Raman spectroscopy. With the aim of analysing liquid samples safely, a new refrigerated Raman cell have been designed, that allows the measurements of a very small amount of sample without risk of ingestion and/or incorporation. Further experiments to characterise aqueous phases containing both, AHA and SO<sub>3</sub>-Ph-BTP, will be presented in the next HYPAR-7.
- IIC has also addressed the development of experimental setup of HPLC and LC-MS methods devoted for analysis of samples of tetrasulfonated BTBP and BTP in water (10 mM, 1 mL water solution), before studying degradation in collaboration with CTU.
- CTU has tested for Am(III) and Eu(III) extraction behaviour for SO<sub>3</sub>-Ph-BTP and SO<sub>3</sub>-Ph-BTBP SANEX systems as function of temperatures, due to the influence of irradiation. Based on the obtained results, thermodynamic parameters (change in entropy and change in enthalpy) were calculated with negative values of  $\Delta H$  and  $\Delta S$ .

## DIFFICULTIES

Most of difficulties reported affecting to task 2.1 are due the situation provokes by COVID-19. As consequence, D2.1 has been postponed until 01-2021:

- Activities related to realistic stability studies of CDTA aqueous phases could not be addressed yet. (CIEMAT)
- No DCs or adducts of BTBP neither BTPen available for experiments yet. (CTU)

- The planned work has not been performed in PPOLIMI and it will be reasonably developed in the next semester. (POLIMI)
- No results due to the coronavirus lockdown. (UREAD)

## ACTION PLAN

- All activities related to task 2.1 must be finished in the next semester. D2.1 has been postponed until 01-2021
- CIEMAT: Quantitative studies of degraded aqueous phases containing AHA or SO<sub>3</sub>-Ph-BTP. Activities regarding realistic stability studies of CDTA aqueous phases.
- CTU: To finish the studies of the temperature dependence of the radiation degradation for both SANEX and CHALMEX extraction systems.
- IIC: Separation of DCs from other Chalmers irradiated samples. Overview NMR, MS and HPLC assignment of DCs isolated.
- POLIMI: HPLC-MS analyses to confirm the identity of the PTD degradation products present in the irradiated PTD solutions and to enable a quantitative analysis, as well as some liquid-liquid extraction tests.
- JUELICH: Further radiolysis data will be evaluated with mTDDGA.
- UREAD: Analysis of the irradiated samples of CyMe<sub>4</sub>-BTBP and BTPPhen in both octanol and cyclohexanol.

## TASK 2.2 DESTRUCTION OF ORGANIC (TASK LEADER: CEA)

### MANPOWER

1 pm realized this semester (CEA).

### MAIN PROGRESSES

All activities related to task 2.2 have been finished and D2.3 Destruction of organics has been written and submitted (UNIPR, CEA 1 pm).

Task 2.2 is now completed

## TASK 2.3 GAS GENERATION (TASK LEADER: POLIMI)

### MANPOWER

0.1 pm were realized this semester (POLIMI).

### MAIN PROGRESSES

All activities related to task 2.3 have been finished or cancel due to some difficulties, there was no additional experimental work.

D2.4 Impacts on process safety of gas generation has been written and submitted (NNL, POLIMI 0.1 pm).

## DIFFICULTIES

Some of difficulties reported affecting to task 2.3 are due the situation provokes by COVID-19:

- Studies related to gas generation ( $H_2$ ) are not possible. Control area was closed in Juelich, so, irradiation was cancelled and the analytical tool for the analysis of radiolysis gas generation is out of order. It is planned to cancel this work and to perform more on Task T21 and T24. (Juelich)

## TASK 2.4 RADIOLYSIS MODELLING (TASK LEADER: CTU)

### MANPOWER

3.4 pm realized this semester (1.4 pm CTU and 2 pm Juelich).

### MAIN PROGRESSES

#### Modelling studies of the radiolysis of lipophilic diglycolamides: (2 pm, Juelich)

The radiolysis mechanism of TODGA and mTDDGA has being further studied using computational methods to enhance the fundamental understanding. For that density functional theory (DFT) calculations with the PBE functional were conducted to obtain reaction profiles for hydrogen abstraction mechanism as main hydrolysis pathway. The Gibbs free energies for which  $\Delta S$  was approximated based on ideal gas formulas insinuate that  $\Delta G$  decreases in both reaction steps, so, the final products are thermodynamically favorable. However, when solvent corrections (n-dodecane) were incorporated for  $\Delta S$ , the second reaction step did not result in a decrease in  $\Delta G$ . The results of implementing this solvent model strongly suggests that, when applying more realistic simulation conditions, this reaction path (hydrogen abstraction on one of the methylene groups next to the ether oxygen) would not be energetically advantageous. This is in agreement with experimental data.

#### Modelling studies of the radiolysis of water soluble diglycolamides: (1.4 pm, CTU)

The theoretical study of TMDGA, TEDGA, Me-TEDGA, and Me<sub>2</sub>-TEDGA dissolved in water has been continued along the two planned pathways: (i) ab-initio QM simulations by DFT method and (ii) conformational analysis by MD followed by statistical analysis of the obtained trajectories.

This semester, based on the raw simulation results, a consolidated quantitative set of molecular stability descriptors has been obtained for four different molecular environment representations: acid-free model,  $H^+$  model,  $H_3O^+$  model, and  $HNO_3$  model. The determined descriptors involve molecular orbitals (HOMO / LUMO), Fukui functions and Fukui charges, partial electronic charges, bond orders, ESP distribution, and stability indicators derived from molecular dynamics. Juxtaposition of the obtained theoretical results with available experimental data has been done.

DFT simulations of degradation reaction pathways and their transient structures were successfully completed on the models including hydrogen abstraction initiated by hydrogen radical. The results have been analyzed and energetics of the reaction trajectories determined.

### ACTION PLAN

CTU: Modifications of the degradation reaction model involving hydroxyl radical will be formulated and tested in attempt to identify correct reaction transients. Possible involvement of reaction products involving alcohol end group, suggested by experimental findings, will be tested, too. Properties of the stability indicators derived from molecular dynamics will be further analyzed. Attempts will be made to combine this class of descriptors related to solution atomic dynamics with the parameters reflecting electronic properties of the tested DGA molecules.

### LIST OF PUBLICATIONS

#### Paper published:

1. P. Distler, K. Stamberg, J. John, L. M. Harwood and F. W. Lewis, *J. Chem. Thermodyn.*, 2020, 141, 105955.
2. P. Distler, M. Mindová, J. John, V. A. Babain, M. Y. Alyapyshev, L. I. Tkachenko, E. V. Kenf, L. M. Harwood and A. Afsar, *Solvent Extr. Ion Exch.*, 2020, 38, 180–193.
3. Afsar, J. S. Babra, P. Distler, L. M. Harwood, I. Hopkins, J. John, J. Westwood and Z. Y. Selfe, *Heterocycles*, 2020, 101, 209–222.
4. Afsar, P. Distler, L. M. Harwood, J. John, J. S. Babra, Z. Y. Selfe, J. Cowell and J. Westwood, *Heterocycles*, , DOI:10.3987/com-18-s(f)71.
5. Petr Distler, Miriam Mindová, Jan John, Vasilij A. Babain, Mikhail Yu. Alyapyshev, Lyudmila I. Tkachenko, Ekaterina V. Kenf, Laurence M. Harwood & Ashfaq Afsar: Fluorinated Carbonates as New Diluents for Extraction and Separation of f-Block Elements, *Solvent Extraction and Ion Exchange*, 2020, Vol. 38, No. 2, 180–193

#### Conferences:

##### Poster presentation:

1. B. Verlinden, P. M. Kowalski, K. Van Hecke, A. Wilden, M. Verwerft, G. Modolo, K. Binnemans, T. Cardinaels. Radiolytic stability of diglycolamide-based extractants for minor actinide separation: Experimental and molecular simulations studies. 10<sup>th</sup> John von Neumann Institute for Computing (NIC) symposium, 27.-28.02.2020, Jülich, Germany.

#### Thesis:

1. Application of quantum simulations for characterizing the stability of organic extraction ligands. MSc Thesis by J. Luštinec (CTU) FNSPE, Prague 2020 (supervisor L. Kalvoda).

#### Chapter:

1. Laura J. Bonales, Iván S.nchez-Garc.a, Hitos Galán, and Joaquín Cobos. “Quantitative Raman spectroscopy (QRS) for nuclear fuel reprocessing applications. A direct method

to analyse acetohydroxamic acid (AHA). 2020, LAMBERT Academic Publishing". LAP. In press. ISBN: 978-3-659-91071-5.

## CONCLUSIONS

After 36 months of GENIORS project it has been reached 100% (+10 synthesis) pm of the 107 pm dedicated to WP2. In general, it has been reported a more than optimal development of the experimental and reporting activities despite the situation provokes by COVID-19 pandemic. Particularly, this semester has been written and submitted two deliverables and 13.6 pm has been reported, distributed between task2.1, task2.2, task2.3 and task2.4. Nevertheless, it must be mentioned that it has been a delay in the supplying of degradation compounds and some experimental work in task 2.1.

*D2.3 Destruction of organic and D2.5 Molecular modelling of particular degradation mechanism of extracting and complexing agents* have been written are already finished; however, *D2.1 Stability and safety studies of hold extraction systems (1 for each CyMe4BTBP, HidroBTBP, TODGA & PTD)* has been postponed to 2021-1-31, when all activities related to WP2 must be finished. Only to those activities involved in irradiation loops work could continue, since there will be included in *D 5.2 Impacts of solvent degradation and recycle on the GANEX process (31-5-2021)*.

## WP3

### INTRODUCTION

The aim of this work-package is to improve the understanding and optimization of the reference chemical systems for advanced solvent extraction separation processes: grouped separation of the actinides (EURO-GANEX), separation of the minor actinides (i-SANEX), or separation of americium only (EURO-EXAM). It includes (i) the understanding of extraction chemistry to support concept process flowsheets (Tasks 3.1 & 3.3), (ii) the acquisition of extraction data to support the conception of process flowsheets (Task 3.2), and (iii) the identification of process options for clean-up of solvents to allow recycle on plant (Task 3.4).

### MANPOWER

The amount of person.month (pm) realized in WP3 for each partner and each semester is summarized in the table below.

	HYPARS						Total Realized	
	1	2	3	4	5	6	(pm)	(%)
CEA	0	4	7	6	0	1	18	<b>151.3%</b>
CIEMAT	1.5	1.5	1	1	1.25	0	6.25	<b>49.2%</b>
CNRS	0	0	4.75	2.2	0.3	0	7.25	<b>120.8%</b>
ICHTJ	3.5	4.6	9	7.45	3.4	3	30.95	<b>73.7%</b>
JUELICH	0	0	3.9	1.8	0	0.5	6.2	<b>70.5%</b>
KIT	6	1.25	1.6	1.7	2.5	2.5	15.55	<b>75.5%</b>
NNL	0.4	0.1	0.88	1.14	0.2	0.47	3.19	<b>65.1%</b>
POLIMI	2	7	9.5	6	1.5	0.3	26.3	<b>128.9%</b>
UNIPR	2	2	3	2	2	2.1	13.1	<b>100.0%</b>
<b>TOTAL</b>	<b>15.4</b>	<b>20.45</b>	<b>40.63</b>	<b>29.29</b>	<b>11.15</b>	<b>9.87</b>	<b>126.79</b>	<b>86.2%</b>

### MAIN RESULTS

#### TASK 3.1 OPTIMISATION OF SYSTEMS (TASK LEADER: POLIMI)

##### MANPOWER

1.6 pm realized this semester (JUELICH, POLIMI, UNIPR).

63.45 pm realized since the beginning of the project, corresponding to 81.3 % of the 78 pm planned for the complete project.

## MAIN PROGRESSES

- D3.1 has been written and delivered
- New batches of PTD were produced in larger scales. Samples were sent to POLIMI to verify their efficiency and selectivity in extraction and to understand which and how much impurities are allowed to be present to make separation feasible in any case.
- Chemical conditions for i-SANEX process conditions using PyTri-Diol (PTD) were investigated in detail by POLIMI, and JUELICH and discussed with NNL and KIT. Flow-sheet calculation using the SX Process software will be conducted at KIT within WP5 using the optimised conditions.

## DIFFICULTIES

- Due to the COVID-19 pandemic, planned i-SANEX optimization studies using PyTri-Diol and a corresponding centrifugal contactor demonstration test had to be postponed.

## TASK 3.2 DISTRIBUTION DATA AND CHEMICAL MODELLING (TASK LEADER: KIT)

### MANPOWER

5.0 pm realized (ICHTJ, KIT)

25.65 pm realized since the beginning of the project, corresponding to 188.6 % of the 13.6 pm planned for the complete project.

## MAIN PROGRESSES

- A batch of 2,6-bis[1-(2-ethylhexyl)-1,2,3-triazol-4-yl]pyridine (PTEH) was synthesised. Distribution data for the extraction of Pu(IV), Am(III), Ln(III) and HNO<sub>3</sub> into PTEH were determined. An equilibrium model for HNO<sub>3</sub> extraction was established.
- The analysis of earlier experiments on the effect of the concentration of T-DGA and of SO<sub>3</sub>-Ph-BTP<sub>4</sub>- in the solvent extraction systems with 0.02 M and 0.04 M T-DGA on the distribution of Eu(III) and Am(III) was carried out. Contradictory conclusions on the presence or absence of heteroleptic complexes of Am<sub>3+</sub> and Eu<sub>3+</sub> cations in the systems have been reached. The experiments must be continued to solve the problem.

## DIFFICULTIES

No delivery of an expected new T-DGA batch by TWENTE to ICHTJ, due to the Covid-19 epidemic.

## TASK 3.3 PHYSICO-CHEMICAL & LOADING (TASK LEADER: CIEMAT)

### MANPOWER

2.7 pm realized (CEA, KIT, POLIMI, UNIPR)

27.15 pm realized since the beginning of the project, corresponding to 79.9 % of the 34 pm planned for the complete project.

**MAIN PROGRESSES**

- D3.3 has been written and delivered
- PTEH loading tests were performed with Pu(IV) and Am(III)
- A large sample (several grams) of PTD was started to be produced to be sent to NNL for loading studies. Preparation was not completed because of lockdown of university labs but the sample is ready and will be sent to NNL as soon as they are ready to receive it.

**DIFFICULTIES**

Delays due to COVID19 lockdown.

**TASK 3.4 SOLVENT CLEAN-UP & RECYCLE (TASK LEADER: NNL)****MANPOWER**

0.57 pm realized (NNL, POLIMI)

10.54 pm realized since the beginning of the project, corresponding to 49.0 % of the 21.5 pm planned for the complete project.

**MAIN PROGRESSES**

- The solvent dose model that has been developed to estimate the dose for the solvent in the EURO-GANEX process has been checked and issued for use by GENIORS partners. This will be used to assess the implications for the solvent quality in the process and how this ultimately affects the solvent management strategy (i.e. clean-up and recycle).
- A review has been carried out to summarise previous experience and identify options that have been employed for the clean-up and recycle of solvent in process flowsheets

**DIFFICULTIES**

Delays to planned secondment of Ivan Sanchez (CIEMAT) to NNL due to COVID-19 travel restrictions, unsure when this can be rescheduled at present

**CONCLUSIONS**

The continuity of actions was maintained in this workpackage. However, some experiments were suspended due to the COVID19 lockout.

Two of the four deliverables planned in this workpackage have been finished in time within this period.

After 36 months, 126.79 pm have been realized within WP3, corresponding to 86.2% of the 147.1 pm planned for the complete project.

## WP4

### INTRODUCTION

The main objectives of the WP solid/liquid interface chemistry is to better understand the phenomena occurring at the solid/liquid interfaces during spent nuclear fuel reprocessing in order to support potential processes. It is divided in two main topics. The first is devoted to dissolution step (Task 4.1). It will be examined not only considering direct interactions between the chemical species coming from the solid and the solution, but also through the development of catalytic reactions at the interface. The second topic is focused on the conversion of actinides by precipitation of original precursors coming from new chemical processes based on wet chemistry routes (Task 4.2). The total man power (pm) dedicated to WP4 (Tasks 4.1 and 4.2) are summarized in the table below

Partner	Total planned	WPASR # 1	# 2	# 3	# 4	# 5	# 6
CNRS/ICSM	38.5	1.6	2.2	7.7	8.4	9.9	7.2
CEA	15.4	0.0	3.0	3.0	1.0	6.0	6.0
SCK.CEN	20.0	2.5	2.5	2.5	2.5	2.5	2.5
UNIMAN	11.0	0.0	0.0	6.0	6.0	0.0	0.0
<b>Total</b>	<b>84.9</b>	<b>4.1</b>	<b>7.7</b>	<b>19.2</b>	<b>17.9</b>	<b>18.4</b>	<b>15.7</b>

### MAIN RESULTS

#### TASK 4.1 STUDY OF THE SOLID/LIQUID INTERFACES DURING DISSOLUTION [1-48] TASK LEADER : CNRS

##### MANPOWER

3.9 pm (CNRS) – 6 pm (CEA) ⇒ Total : 9.9 pm

##### MAIN PROGRESSES

Three main actions have been developed in the field of task T4.1.

##### **Multiparametric study of the dissolution of (U,Ce)O<sub>2</sub> and (U,Ln)O<sub>2-x</sub> solid solutions – CNRS/ICSM**

In order to develop the multiparametric dissolution tests, the preparation then characterization of a large defined panel of uranium-lanthanide solid solutions has begun in 2018. Several kinds of powdered and sintered samples were prepared with this aim.

In order to study the impact of the lanthanide mole loading on the chemical durability of U<sub>1-x</sub>Nd<sub>x</sub>O<sub>2-y</sub>, U<sub>1-x</sub>Gd<sub>x</sub>O<sub>2-y</sub> and U<sub>1-x</sub>Ce<sub>x</sub>O<sub>2</sub>, several dissolution tests were performed in static conditions. Around 100 mg of powder heated at 1000°C were put in contact with 20 mL of 2 mol.L<sup>-1</sup> HNO<sub>3</sub> at room temperature (or at 60°C) for few days in high-density polytetrafluoroethylene (PTFE) vessels. During this time, aliquots of 300 µL were regularly taken off and replaced by the same volume of fresh nitric acid solution to maintain a constant volume of solution.

For homogeneous samples, uranium and cerium were released almost congruently during all the dissolution tests. Indeed, at room temperature, the evolution of all the normalized mass losses

exhibited a similar behavior with a two-steps evolution. The first one was associated to surface driving reactions. During the second step (catalyzed controlling mechanism), the evolution of the standardized mass loss then became non linear, and corresponded to the fast release of the cations in solution. At room temperature, the normalized dissolution rates obtained for uranium-lanthanide solid solutions were found to be higher than for the pure end members, with slight variations versus the chemical composition. When making the dissolution tests at higher temperature (i.e. 60°C), the first step was not observed anymore. At this temperature, the full dissolution of the materials was obtained after less than 15 minutes, with a significant decrease of the normalized dissolution rates when incorporating lanthanide elements in the materials.

For heterogeneous sintered samples, the dissolution became incongruent, with a preferential release of cerium compared to uranium, surely due to the presence of Ce(III) in the prepared pellets. Simultaneously, the chemical durability of the samples was decreased compared to homogeneous samples. Additionally, the duration of the induction period was shortened and then the samples were dissolved more rapidly.

### ***Innovative dissolution routes for highly plutonium doped (U,Pu)O<sub>2</sub> and (U,Pu,MA)O<sub>2</sub> samples – CEA***

During this semester, the writing of an article has been performed to be submitted during the next semester. Also, the writing of the PhD manuscript associated to this work is under progress. In the same time, the writing of the deliverable D4.2. *Innovative dissolution routes for highly plutonium doped (U,Pu)O<sub>2</sub> and (U,Pu,MA)O<sub>2</sub> samples* is under progress. During the next semester; the effect of the energy of grinding on dissolution linked to the quantity of crystalline defects brought by the grinding, will be examined. Moreover, the dissolution kinetics enhancement mechanism will be elucidated (especially the role of Ce<sup>3+</sup>/dislocations). Couplings between grinding and dissolution will be carried out.

### ***Dissolution and leaching investigations on CeO<sub>2</sub> and UO<sub>2</sub> – UNIMAN***

The work performed in the reporting period can be divided into three main areas.

- Development of metal oxide materials suitable as nuclear fuel and spent fuel models

The sample matrices have been fully prepared awaiting further studies.

- Dissolution and leaching investigations

Structural characterization of the above is mostly complete, though complicated due to the active nature of the samples mean that  $\alpha$  irradiation of these samples at DCF cannot be conducted. Dissolution studies will be undertaken upon completion of characterization. Techniques being used include XRD, SEM, TRLS, with Raman analysis pending. Further data interpretation is pending the return to technical staff following COVID-necessitated university closure.

- Dissemination

The project research has been presented several times at the university of Manchester. All work is being finalised for publication.

For the next semester, leaching/dissolution studies of the U- and Th-containing samples are to be investigated under simulated SNF storage conditions, as previously described. The previously described results are to be published when data interpretation can be completed.

## **DIFFICULTIES**

### **UNIMAN**

Some challenges have been encountered in the availability of XPS, XANES and XAFS techniques due to the movement of analytical equipment and personnel within the university, and the necessary

containment requirements for handling active materials, though XPS measurements have been undertaken. The Covid-19 pandemic has resulted in the complete shutdown of the university campus and thus the total cessation of laboratory work. Additionally, technical staff have been furloughed and are hence unavailable to assist with data interpretation. The final characterization and following dissolution studies will be carried out once a return to the university is feasible. Additionally, the PDRA associated with this project has now officially finished (as his funding has run out), but he is able to complete the project in his spare time as he has moved onto another project in the university.

## CEA

Problem with the milling device + Covid.

## CNRS/ICSM

Due to the Covid-19 pandemic, all the experiments have been stopped by mid march and the laboratories have been closed. Most of the on-going long-term dissolution tests have been stopped and have to be duplicated after re-opening of the labs. Consequently, the operando monitoring of the solid/liquid interface at the microscopic level has failed. New dissolution tests should start by the end of June or by mid-July depending on the authorization to enter the labs again. *Consequently, the deliverable D4.1 "Understanding the evolution of an interface during dissolution of actinide oxide materials by macro/microscopic approaches combination" should be delayed from end of September, 2020 to end of December, 2020 (i.e. by 3 months).*

## ACTION PLAN

### CNRS/ICSM

Dissolution tests were developed on various powdered and sintered samples of  $U_{1-x}Nd_xO_{2-y}$ ,  $U_{1-x}Gd_xO_{2-y}$  and  $U_{1-x}Ce_xO_2$  solid solutions in  $2 \text{ mol.L}^{-1} \text{ HNO}_3$  at room temperature. They will be completed at  $60^\circ\text{C}$ . Moreover, complementary operando experiments (microscopic approaches), which have been delayed due to the Covid-19 pandemic. They will be monitored by ESEM in order to underline the preponderant mechanism occurring at the interface during dissolution tests.

### CEA

During this semester, the writing of an article has been performed to be submitted during the next semester. Also, the writing of the PhD manuscript associated to this work is under progress. In the same time, the writing of the deliverable D4.2. *Innovative dissolution routes for highly plutonium doped (U,Pu)O<sub>2</sub> and (U,Pu,MA)O<sub>2</sub> samples* is under progress and should be submitted, on time, by the end of February, 2021.

### UNIMAN

Leaching/dissolution studies of the U- and Th- containing samples are to be investigated under simulated SNF storage conditions, as previously described.

## LIST OF PUBLICATIONS

### Int. Conference Oral:

New insights in the description of the dissolution of actinide dioxides : better understanding for their reprocessing, N. Dacheux, INSPYRE First Summer School, Delft, 13-17 mai, 2019 / *Given*

Contribution of the coupling milling / dissolution on the dissolution of oxides, J. Hidalgo, P. Roussel, T. Delahaye, G. Leturcq, J.L. Rouviere, EMRS Spring Meeting 2019, Nice, 27-31 mai 2019 / *Given*

## TASK 4.2 STUDY OF THE SOLID/LIQUID INTERFACE DURING CONVERSION [1-48] TASK LEADER : SCK.CEN

### MANPOWER

3.3 pm (CNRS/ICSM) + 2.5 pm (SCK.CEN) ⇒ Total : 5.8 pm

### MAIN PROGRESSES

Four main actions have been developed in the field of task T4.2.

#### ***Studies of non-powder routes for the synthesis of MOX fuels materials, potentially bearing minor actinides and blanket fuel materials – SCK.CEN***

Within this reporting period previously presented results were wrapped up and summarized in manuscripts, in total 3 publications were compiled. Those cover the fabrication of  $U_{1-y}Ce_yO_{2+x}$  microspheres by internal gelation, using trivalent and tetravalent Ce precursors (HYPAR1-3), accepted to Journal of Nuclear Materials and the In-situ study of aforementioned particles during thermal treatment by TG-DSC and HT-SEM (HYPAR5), submitted to Journal of Nuclear Materials, (now in revision). A third paper dealing with the fabrication of Ce-doped ADU by urea decomposition (HYPAR4) is in preparation. During next semester, data processing of thermal decomposition on Ce-doped ADU powder and microspheres will be done. Moreover, finalizing manuscripts on (1) hydrolysis of Nd- & Ce-doped ADU by thermal decomposition of urea and (2) thermal decomposition study of Nd- & Ce-doped ADU powder and microspheres is also expected.

#### ***Hydrothermal precipitation of uranium oxides for simplified fuel fabrication – CNRS/ICSM***

The direct precipitation of uranium oxides has been undertaken under hydrothermal conditions through the *in situ* conversion of uranium oxalate. Below 180°C,  $U(C_2O_4)_2 \cdot nH_2O$  was formed whereas  $UO_{2+x} \cdot nH_2O$  was prepared above this temperature. Moreover, HERFD-XANES showed that the O/U stoichiometry was affected by the temperature and typically ranged from 2.4 up to 210°C to 2.1 between 220 and 250°C. SEM observations revealed the loss of the classical square platelet shape of the oxalate, while the evaluation of the residual carbon and water contents led to values significantly lower than that usually obtained through thermal conversion. Additionally, the pH control allowed to optimize the uranium precipitation yield and to orientate the morphology towards agglomerated microspheres. From the multiparametric study of the hydrothermal conversion, crystalline  $UO_{2+x} \cdot nH_2O$  samples were obtained after only 1 hour of heat treatment at 250°C (5 hours being necessary to improve the crystallinity of the powders). Nevertheless, the samples obtained after 1h were found to be highly oxidized ( $O/U \approx 2.6$ ), which suggested that the conversion mechanism should be based on the oxidative decomposition of the initial U(IV) oxalate, then on the hydrothermal reduction of uranium thanks to organic species in solution. Finally, first results concerning the preparation of  $U_{1-x}Ce_xO_2$  mixed oxides were obtained and showed that the recovery of uranium was quantitative through a heat treatment of 24 hours at 250°C and pH = 5 whereas cerium recovery depended on the cerium content in the starting mixtures could be obtained. Also, preliminary studies regarding the sintering capability of the powders have been undertaken thanks to dilatometry tests.

***Innovative precursors for morphology-controlled  $UO_2$  and  $(U,Ln)O_2$  oxides – CNRS/ICSM***

$UO_{2+x}.nH_2O$  microspheres were obtained through hydrolysis of uranium(IV) in the presence of aspartic acid under hydrothermal conditions (160°C). A multi-parametric study involving time, temperature, concentration of the reactants was then undertaken. It showed that a 50% excess in aspartic acid led to monodisperse powders. The addition of mechanical stirring during the hydrothermal process allowed to accurately control the average diameter of the particles produced (400 – 2500 nm range). For all the conditions tested, the characterization of the powders showed the formation of fluorite type  $UO_{2+x}.nH_2O$  samples with traces of residual organics at the surface. Both water and residual organics were eliminated by heating at 600°C. This latter did not alter the shape of the particles and allowed the preparation of size-controlled  $UO_{2+x}$  microspheres. Complementary FIB experiments further confirmed the absence of porosity within these particles. Finally, preliminary tests concerning the synthesis of mixed  $(U,Ce)O_{2+x}$  particles were undertaken and showed the formation of microspheres up to 10 mol.% in cerium. The first dilatometric experiments aiming to evaluate the sintering capability of these solids are now under progress.

***Conversion of uranium nitrate into uranium oxide by Solution Combustion Synthesis –CNRS/ICSM***

The solution combustion synthesis (SCS reaction) of metal nitrate to oxide is a self-propagating reaction of an organic fuel with a metal nitrate dissolved in water. In a first stage, this reaction was employed with an actinide surrogate element. The conversion of  $Gd(NO_3)_3$  to  $Gd_2O_3$  was obtained with glycine and citric acid as fuel, for a heating temperature of 300°C. Under these conditions, for a fuel /  $Gd(NO_3)_3$  stoichiometric ratio, the monoclinic phase  $Gd_2O_3$  was obtained with a high specific surface area (10-20  $m^2/g$ ), a small amount of residual carbon and a good crystallinity. The ignition of the precursors leading to the conversion nitrate / oxide, was observed at a temperature of about 210°C. The conversion of uranyl nitrate into  $UO_2$  was obtained using citric acid or glycine as fuel, for a richness (ratio  $UO_2(NO_3)_2$  /fuel), respectively equal to 1 and 1.7. For the other richness values, a mixture of  $U_3O_8$  and  $UO_{2+x}$  was obtained. The reaction was successfully extended to the  $U_xCe_{1-x}O_2$  solid solutions. The powders obtained have interesting characteristics (15-25  $m^2/g$ ), and their sintering was successfully carried out.

**DIFFICULTIES**

**CNRS/ICSM**

Due to the Covid-19 pandemic, all the experiments have been stopped by mid march and the laboratories have been closed. Concerning the task T4.2., several experiments have been delayed. *From that we know now, they should not induce any delay for the deliverable D4.4. “ Impact of the precursor “history” (nature, structural, microstructural and morphological parameters) during the conversion and sintering to actinide based dioxide materials [month 45]”*

**ACTION PLAN**

**SCK.CEN**

During the next semester, the data processing of a manuscript on the thermal decomposition of Nd- and Ce-doped microspheres and ADU powder will be performed.

**CNRS/ICSM**

Final experiments on the precipitation of  $U_{1-x}Ce_xO_{2-y}$  mixed oxides under hydrothermal conditions. Finalization of the deliverable D4.1 *Understanding the evolution of an interface during dissolution of actinide oxide materials by macro/microscopic approaches combination* [month 44].

Final experiments on the sintering of uranium oxides obtained through hydrothermal conversion of oxalate studied through dilatometry and establishment of sintering map. Finalization of the deliverable D4.4 *Impact of the precursor "history" (nature, structural, microstructural and morphological parameters) during the conversion and sintering to actinide based dioxide materials* [month 45].

## LIST OF PUBLICATIONS

### Publications:

**Hydrothermal conversion of uranium(IV) oxalate into oxides : a comprehensive study**, J. Manaud, J. Maynadié, A. Mesbah, M.O.J.Y. Hunault, P. Martin, M. Zunino, D. Meyer, N. Dacheux, N. Clavier, *Inorg. Chem.*, 2020, 59, 3260.

**Fabrication of Nd- and Ce-doped  $UO_2$  microspheres via internal gelation**, C. Schreinemachers, G. Leinders, G. Modolo, M. Verwerft, K. Binnemans, T. Cardinaels, *J. Nucl. Mater.*, 2020 (*in press*).

**Structural changes of Nd- and Ce-doped ammonium diuranate microspheres during the conversion of  $U_{1-y}Ln_yO_{2\pm x}$** , C. Schreinemachers, G. Leinders, R. Podor, J. Lautru, N. Clavier, G. Modolo, M. Verwerft, K. Binnemans, T. Cardinaels, *J. Nucl. Mater.*, 2020 (*submitted*).

## CONCLUSIONS

Several complementary ways of preparation of precursors were already developed or are now under progress. They were (are) able to provide a large variety of oxide based materials (Ce, U-Ce, U-Ln, U doped with FP) exhibiting various compositions, microstructures, crystal defects due to milling or to radiation damages. This spread panel of materials allowed to develop various dissolution experiments in order to access multiparametric expression of the dissolution rates. Only few difficulties (mainly due to Covid-19 pandemic) are encountered by the partners, especially for T4.1.

## WP5

### TASK 5.1

#### MANPOWER

- Jülich: 0 pm
- CNRS: 0 pm
- CIEMAT: 4.5 pm
- ULEEDS: 0 pm
- ULANC: 0 pm
- CEA: 3 pm

#### MAIN PROGRESSES

- ULANC:
  - RDC extraction data has been analysed using different models to determine the roles played by chemical complexation and physical mass transfer.
  - Aspects of the mass transfer/chemical reaction model has been addressed:
    - Complexation reaction stoichiometry has been relaxed from the assumed 1:1 stoichiometry by including a parameter  $\gamma$ .
    - The assumed interfacial concentration of the complex of 0 has been relaxed and a non-zero value allowed
  - Curve-fitting of extraction rate vs RDC rotation speed data for the i-SANEX analogue Ce(III)/TODGA RDC extraction system has been performed allowing for the determination of  $[C_i]$  and other key parameters.
  - A sensitivity analysis based on the known parameters of complexation stoichiometry and diffusivity of the complex in the aqueous phase has been performed.
- CEA:
  - Preliminary kinetics data acquisition were performed with microfluidics device for  $10^{-3}$  M Eu(III), Fe(III) and Gd(III) extracted from 3 M  $\text{HNO}_3$  by 0.5M mTDDGA in TPH
- CIEMAT:
  - Continued work with the irradiation loop at Náyade facility
    - Design improvement
    - First EURO-GANEX test loop
  - Preparation of two papers and D5.2

#### ACTION PLAN

- JÜLICH:
  - Complete planned i-SANEX optimisation studies and centrifugal contactor demonstration test in collaboration with POLIMI and UNIPR.
- ULANC:
  - Curve-fitting of the  $[C_i]$  variable boundary condition model to the RDC dataset for i-SANEX analogue Ce(III)/TODGA extraction system and sensitivity analysis.
  - Import more RDC extraction data into the model for parameter estimation

- Commence RCD studies of Ln(III)/mTDDGA extraction system
- CEA:
  - Kinetics data acquisition: Increase the cation concentration in the aqueous stream (1, 10 and 20 g L<sup>-1</sup>) and/or with slower velocities. Determination of mass transfer coefficients of Eu(III) in the stripping conditions of new Euro-GANEX (PTD solution and mTDDGA solvent) with the microfluidics device or the single drop technic.
  - Model development
- CIEMAT: Depending on when CIEMAT facilities will open:
  - Measurement and analysis of the data from the Euro-GANEX test loop irradiation
  - Additional experiments to understand and confirm Euro-GANEX test loop results.

## TASK 5.3

### MANPOWER

ULEEDS: 6 pm

### MAIN PROGRESSES

- ULEEDS:
  - Developed a working CFD model of a simplified ACC configuration using an established standard multiphase modelling technique (i.e. VoF)
  - A more accurate CFD model of simplified ACC configuration has been developed
  - PhD Project on PSEC modelling is complete, and student is preparing his thesis

### DIFFICULTIES

- ULEEDS:
  - Some delays due to IT issues
  - No delays due to Covid-19

### ACTION PLAN

Complete ACC model and publish paper describing the technique

## LIST OF PUBLICATIONS

### CIEMAT

Sánchez-García, H. Galán, J.M. Perlado and J. Cobos. “Development of experimental irradiation strategies to evaluate the robustness of TODGA and water-soluble BTP extraction systems for advanced nuclear fuel recycling” Radiation Physics and Chemistry 2020, Submitted

### ULEEDS

Theobald, Daniel W.; Hanson, Bruce ; Fairweather, Michael ; Heggs, Peter J. “Implications of hydrodynamics on the design of pulsed sieve-plate extraction columns: A one-fluid multiphase CFD model using the volume of fluid method”, March 2020, Chemical Engineering Science, Elsevier Ltd, Volume 221

## WP6

### INTRODUCTION

The objectives of WP6 are to optimise the efficiencies and safety of separation processes developed under the SACSESS project (*i.e.* i-SANEX, EURO-GANEX, EXAm, CHALMEX) The main emphasis is on process development through flowsheet testing. WP6 focuses on optimisation of the reference separation processes, particularly where significant simplification is possible or replacement of non-CHON ligands by CHON molecules can be proposed. It also includes extension of process envelopes to more challenging GenIV feeds and integration of the minor actinide SX cycles with upstream and downstream stages, particularly where interfaces may cause issues.

### MAIN RESULTS

#### MANPOWER

A total of 16.6 person-months has been reported split into 11.6 person-months for Task 1 (CHALMERS, JUELICH, KIT, NNL), and 5 person-months for Task 2 (JUELICH, UNIPR). This represents a slight increase on semester 4 which reported 15.6 person-months but still less than semester 4 (17.3 person-months). Whilst this may still reflect decisions taken at the Antwerp workshop that GENIORS focuses more on basic chemistry of the extraction processes and less on flowsheet testing due to the lack of basic knowledge of some of the extractants, e.g. m- TDDGA, the impacts of COVID-19 have also delayed progress by shutting down laboratory work.

### TASK 6.1: HOMOGENEOUS RECYCLING

#### MAIN PROGRESSES

##### PLUTONIUM LOADING EXPERIMENTS WITH MTDDGA

The current EURO-GANEX flowsheet is based upon a solvent system of 0.2M TODGA / 0.5M DMDOHEMA in OK. Although the system was shown to work well in a hot test, it is more complicated to maintain the composition of a two extractant system in a process and the maximum Pu loading of the solvent decreases with increasing nitric acid concentration. The modified diglycolamide, mTDDGA, has been shown to offer the potential to simplify the solvent system, while capable of achieving high Pu loadings without 3rd phase formation [1] . Therefore, it is essential to understand the third phase boundary with regard to the Pu loading of the solvent. Formation of a 3rd phase can depend on several factors, including temperature, extractant concentration, diluent, metal (Pu) loading and acidity. A series of batch tests have been performed to assess the effect of mTDDGA concentration, nitric acid concentration and Pu loading upon third phase formation :

[mTDDGA]: 0.1 to 0.5M

[Pu]: 0 to 60 g/l

[HNO<sub>3</sub>]: 1 to 7M

Aqueous solutions were prepared by dilution of the concentrated stock of Pu nitrate and nitric acid to obtain the desired concentration. 0.5ml of the aqueous phase was contacted with an equal volume of mTDDGA in OK (0.1 to 0.5M) for 15 minutes. Samples were allowed to settle and the presence of 3rd phase was recorded. All batch tests were performed with the cis isomer of mTDDGA obtained from Technocomm Ltd.

Results from these batch tests are presented in Figure 1, which shows the presence / absence of 3rd phase (or precipitates) in samples at varying nitric acid concentration, Pu loading and mTDDGA concentration. In 0.5M mTDDGA, the high Pu loading produced a very dark, viscous organic phase that made it difficult to observe the presence of a third phase at the aqueous / organic interface. In these batch tests third phase formation was not apparent at Pu loading up to 55 g/l with an initial aqueous nitric acid concentration of 5M. Similar high loadings were observed in 4 to 7M HNO<sub>3</sub> without third phase formation. This is also in agreement with recent data reported by KIT. The original studies with mTDDGA reported observation of precipitation at Pu loading of 48 g/l, however this was probably due to the effect of the diluent as these initial studies used ndodecane rather than OK. At these high Pu loadings the solvent phase is viscous and phases are slow to disengage under gravity. The high Pu loading suggests that Pu is present predominantly as a 1:2 complex with mTDDGA rather than a 1:3 complex. A loading of 55 g/l represents a solvent loading of 92% assuming a theoretical maximum based on the formation of a 1:2 complex.

These results are significantly higher than the original EURO-GANEX solvent which reported third phase formation to occur at a Pu loading of 20 g/l with an initial aqueous nitric acid concentration of 5M. In addition, the maximum Pu loading of the EURO-GANEX solvent decreases with increasing nitric acid concentration, from 35 g/l at 3M to 2.5 g/l at 7M [2].

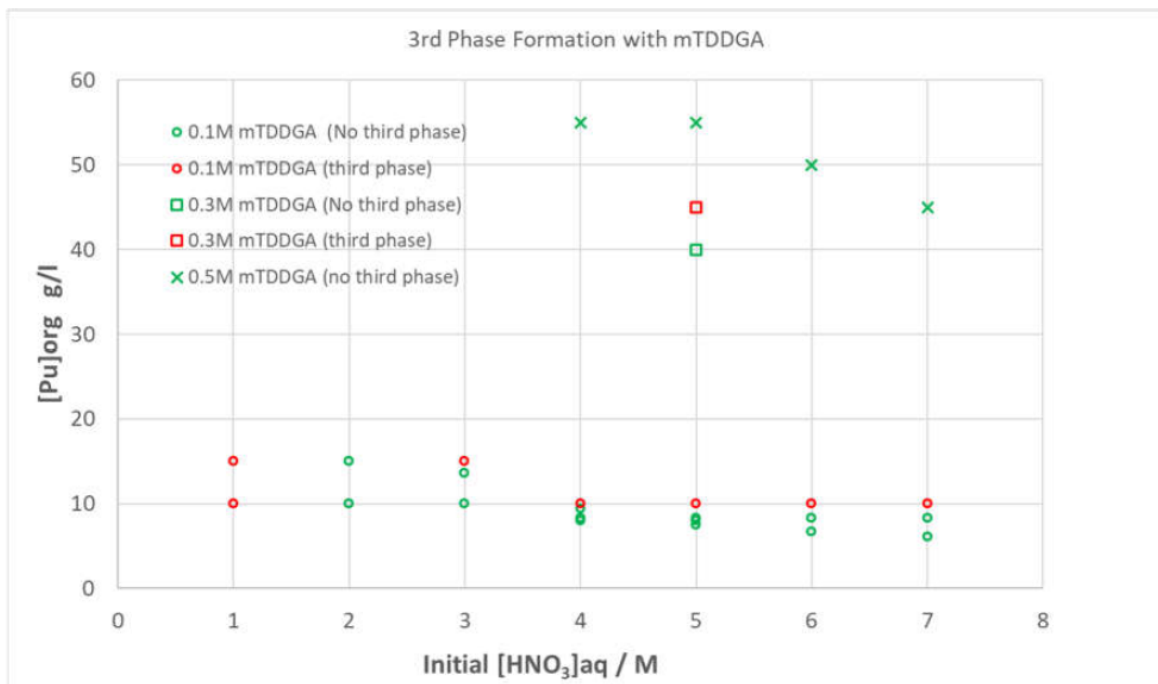


**Figure 1. Pu loading and third phase formation with mTDDGA**

Due to the high solvent loadings that could be achieved with 0.5M mTDDGA and the resulting high viscosity of the loaded solvent, further batch tests were performed at lower mTDDGA concentration. At 0.3M mTDDGA it was possible to obtain a Pu loading up to 40 g/l without precipitation or 3rd phase

formation. Formation of a precipitate was observed upon increasing the Pu loading to 45 g/l. It is noted that this loading actually exceeds the Pu concentration required for complete saturation of the solvent as a 1:2 complex with mTDDGA.

Further batch tests performed with 0.1M mTDDGA in OK showed a difference in precipitation / 3rd phase formation compared to the tests with 0.3M and 0.5M mTDDGA. With the lower extractant and Pu concentration the presence of a narrow dark band at the aq./org interface was readily detected at the onset of 3rd phase formation. It is apparent that the third phase behaviour of this system is dependent upon the initial aqueous nitric acid concentration. With an initial nitric acid concentration above 4M the maximum Pu loading that can be attained remains constant at approximately 8 to 9 g/l. This suggests that the onset of 3rd phase formation occurred as the Pu concentration exceeded the limit for the formation of the 1:3 complex. The onset of third phase formation changes as the nitric acid concentration decreases below 4M. With an initial aqueous nitric acid concentration < 4M it was observed that the solvent could tolerate higher Pu loading prior to 3rd phase formation, increasing to 13.6 g/l for 3M HNO<sub>3</sub> and no 3rd phase was observed with a Pu loading of 15 g/l at 2M HNO<sub>3</sub>. However, upon decreasing the initial nitric acid concentration to 1M, precipitation was observed at Pu concentration of 10g/l and 15g/l.

The results confirm that it is possible to achieve high Pu loading in this solvent system without precipitation occurring, and the high loadings imply the formation of a 1:2 complex with mTDDGA. These results also demonstrate that it is possible to achieve high Pu loading at a lower concentration of mTDDGA, up to 40 g/l with 0.3M mTDDGA. Compared with the original EURO-GANEX solvent this system does not exhibit the same rapid decrease in loading capacity with increasing nitric acid concentration. However, a difference in the 3rd phase formation behaviour was observed with 0.1M mTDDGA. In this case, onset of 3rd phase formation was observed when the Pu loading exceeds the concentration required for the formation of the 1:3 complex. Interestingly, this was not observed for 0.3M and 0.5M mTDDGA and does present the question whether the dark colour of the loaded organic phase masked the presence of the third phase at the higher extractant concentration.

Further batch tests are planned to:

- Investigate whether any 3rd phase formation can be observed when the Pu concentration exceeds the limit for formation of 1:3 complex in 0.3M mTDDGA and 0.5M mTDDGA
- Assess effect of the trans-mTDDGA upon the Pu loading of the solvent.

## CHALMEX STUDIES

Extraction kinetics were investigated for extraction from a simulated PUREX raffinate. As can be seen in Figure 2, the elements extracted by TBP (U, Pu (Np)) reach equilibrium within 10 minutes, as expected from PUREX chemistry. Americium and curium distribution ratios, however, show an increase in distribution ratios until 10 minutes, after which the distribution ratios decreases until equilibrium is reached after about 90-100 minutes. Despite the equilibrium distribution ratios of below 1 for both americium and curium, their extraction behavior show that industrial operation below equilibrium would be beneficial for the CHALMEX process. The distribution trends also suggest that both americium and curium are competed out by the extraction of another element.

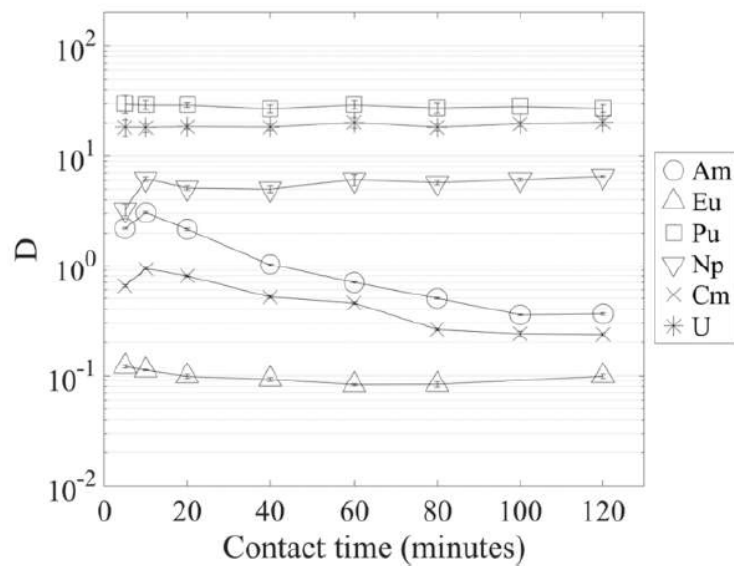


**Figure 2. The distribution ratio, D, of the actinides and europium with time. Extraction was done with 10 mM CyMe4-BTBP in 30%vol TBP and 70%vol FS-13 from a simulated PUREX raffinate.**

By considering both the concentration in the PUREX raffinate and the extraction trends it was found that the most likely cause of this was the extraction of nickel. The extraction of Pd, Ag and Cd can be seen in Figure 3 and Ni, Zr and Mo is shown in Figure 4. Here it becomes apparent that the extraction of silver and palladium reach equilibrium within 10 minutes, and these elements can thus not be the cause of the decreasing D(Am) and D(Cm) with time. Cadmium extraction reaches equilibrium after approximately 40 minutes. Furthermore, the elements present in high abundance, such as molybdenum and zirconium, reaches extraction equilibrium after 60 minutes of contacting. Nickel, as americium and curium, reaches equilibrium after about 90- 100 minutes.

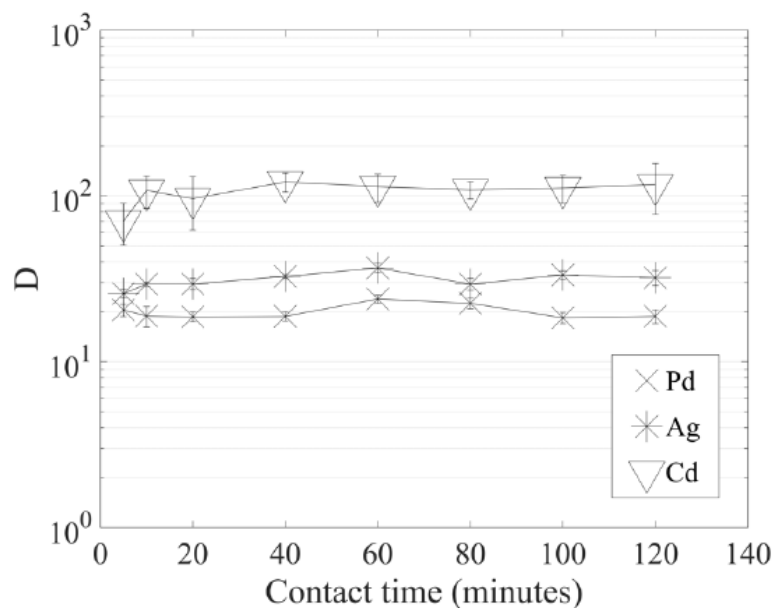


**Figure 3. The extraction of palladium, silver and cadmium with time. The solvent was 10 mM CyMe4-BTBP in 30% TBP and 70% FS-13.**

The extraction of the actinides and fission products were investigated as a function of nitric acid concentration, and the results can be seen in Figure 5 and Figure 6.  $D(\text{Am})$  increases with nitric acid concentration until  $[\text{HNO}_3]=2.5\text{ M}$  where  $D(\text{Am})$  reaches its maximum with  $D=46$ . At higher acid concentrations,  $D(\text{Am})$  decreases indicating competition with acid extraction. Curium shows the same trend for distribution ratios as americium, with just slightly lower  $D$ -values.  $D(\text{Cm})_{\text{max}}$  is also found at  $[\text{HNO}_3]=2.5\text{ M}$ , with  $D=23$ . Plutonium distribution ratios agree with expected trends from the PUREX process, with increasing distribution ratios with increasing nitric acid concentration. The distribution ratio of neptunium increases with nitric acid concentration until  $[\text{HNO}_3]=2\text{ M}$ , after which it reaches equilibrium. Europium, not unexpectedly, follows same trends as americium and curium, although the distribution ratio remains under 1 for all nitric acid concentrations.

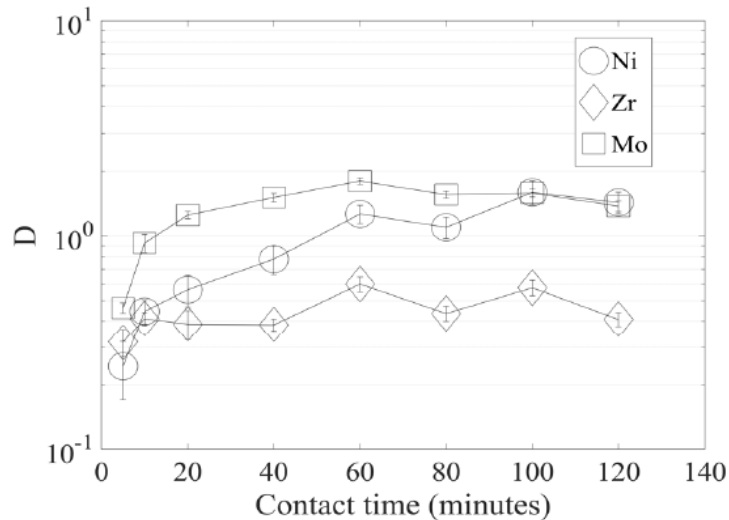


Figure 4. The extraction of nickel, zirconium and molybdenum with time. The solvent was 10 mM CyMe4-BTBP in 30%vol TBP and 70%vol

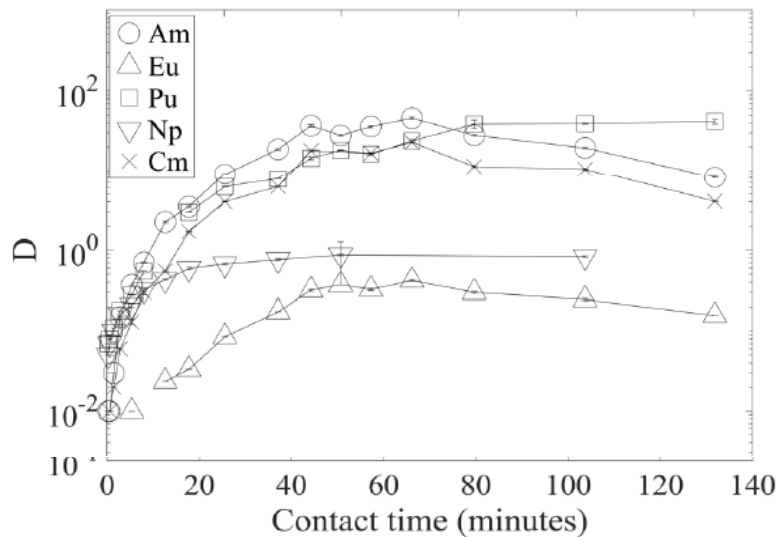


Figure 5. The distribution ratio ( $D$ ) of Am, Eu, Pu, Np and Cm as a function of nitric acid concentration.

The extraction of relevant fission products with  $D>0.1$  is shown in Figure 6, with the exception of Ag and Cd which both had  $D>>100$ . The distribution ratios of nickel, molybdenum and palladium remain  $<1$  for nitric acid concentration 1.5 M. From nitric acid concentration 0.7 M, the distribution ratio of zirconium, molybdenum and palladium are all seen to increase proportionally with the increase in acid concentration. The nickel distribution however shows an unexplained jump in distribution ratios from

0.12 to 25 for 1.5 and 1.75 M nitric acid concentration respectively. All other fission products (including the lanthanides) had distribution ratios below 0.1.

The effect of the complexing agents bimet and mannitol on the extraction was also further investigated, along with two novel complexing agents referred to as agent 10 and 13 respectively. The former (bimet and mannitol) were reported in HYPAR5 for extraction trace level metals, while the two latter will be reported here. Agent 10 and agent 13 were developed for the masking of palladium and nickel but was reported to also efficiently suppress silver extraction. Agent 10 and agent 13 were both combined with 0.2 M mannitol for the suppression of zirconium and molybdenum, as shown in HYPAR 4.

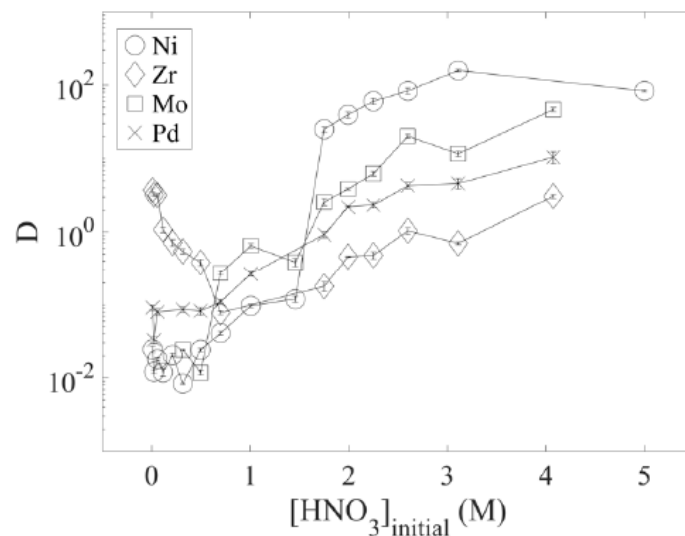


Figure 6. The distribution ratio, D, of nickel, zirconium, molybdenum and palladium as a function of nitric acid concentration.

Figure 7 shows the most effective masking agents and their suppression of the most worrisome fission products. In addition to these, EDTA, HEDTA, DTPA and CDTA have been investigated. Despite promising results reported by Sypula et al4, most of these masking agents did not show any significant reduction in most of the fission product distribution ratio. CDTA however reduced D(Cd) from > 1000 to D(Cd)~1.6, and D(Cu) from ~ 70 to D(Cu) ~ 13. Agent 13 appears to have the biggest effect on the fission products: the distribution ratios of silver, nickel and palladium are all significantly reduced. Only D(Pd) is however reduced to below 1. For both masking agent 10 and 13 the distribution ratio of zirconium is reduced, which is beneficial due to the high relative concentration of zirconium in spent nuclear fuel. Agent 10 does however not have any effect on the silver extraction, nor the palladium extraction. On the contrary, nickel extraction is increased from the pristine system.

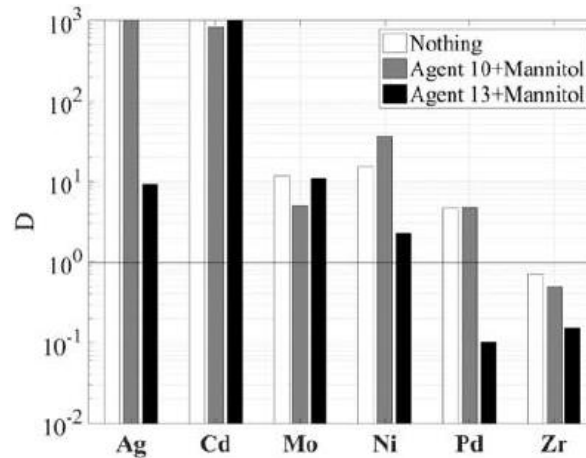


Figure 7. The distribution ratios of silver, cadmium, molybdenum, nickel, palladium and zirconium in systems without and in presence of masking agents.

The effect on the actinides is also profound, as seen in Figure 8.  $D(\text{Am})$  is significantly increased and it is above 10 in all systems. The most concerning effect is seen for the europium distribution ratio. In the pristine system it is 0.25, while in systems with agent 10 and agent 13 the distribution ratio is 1.28 and 1.32 respectively. Although the SF factor is maintained for the actinides, the high distribution ratio for europium is not promising.

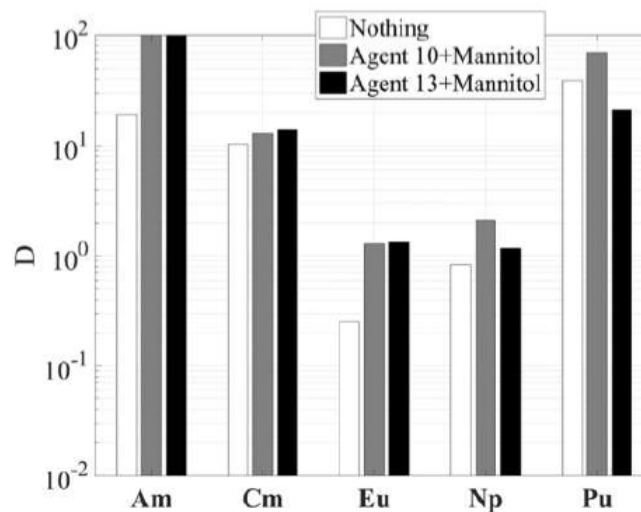


Figure 8. Distribution ratio of the actinides, and europium, in systems without and in the presence of masking agents.

Figure 9 shows the distribution ratios of the most extracted fission products as a function of nitric acid concentration in the presence of mannitol and agent 10 or agent 13 respectively. For both masking agent 10 and 13, the distribution ratios of zirconium and molybdenum increases until nitric acid concentration of 3 M. At higher acid concentrations, the distribution ratios decrease. As molybdenum and zirconium are both suppressed by mannitol, similar trends in both systems are expected. In the presence of masking agent 10 (Figure 9 a)

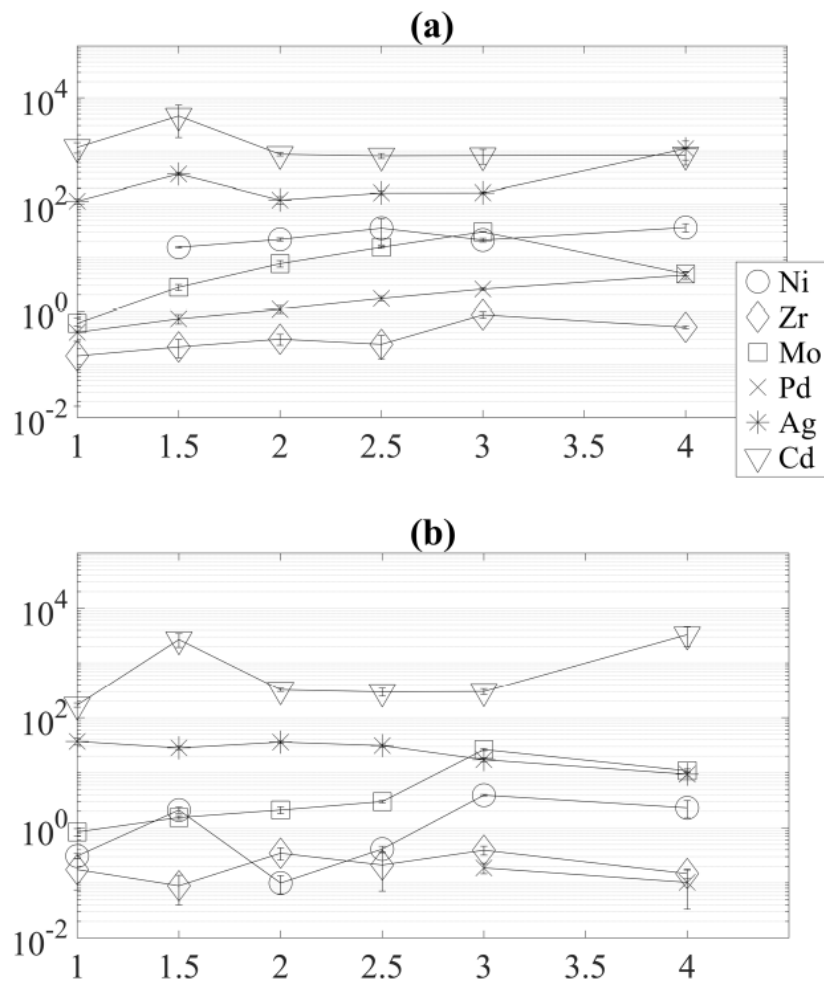


Figure 9. The distribution ratios of nickel, zirconium, molybdenum, palladium, silver and cadmium as a function of nitric acid concentration in the presence of a) Masking agent 10 and b) Masking agent 13.

The effect of the different masking agents was also investigated for extraction from a simulated PUREX raffinate. As was shown in earlier HYPARs, the standard solvent of 10 mM CyMe4-BTBP co-extracted several fission products, which reduced the actinide extraction to  $D < 1$ . It was thus also of interest to see what effect simply increasing the CyMe4-BTBP concentration have on the actinide extraction.

Considering Figure 10, one can see that increasing the ligand concentration increases the extraction of molybdenum and nickel in particular. It has little effect on the other fission products. Addition of various masking agents, however, has a profound effect on several fission products. The molybdenum extraction is decreased for all masking agents showing that molybdenum is suppressed by all masking agents, not only mannitol. Silver extraction is reduced significantly also for silver, but only the bimetal and mannitol combination reduces  $D(\text{Ag})$  to below 1.  $D(\text{Ni})$  is reduced by both agent 10 and 13, although  $D(\text{Ni}) > 10$  in all cases. Only bimetal and mannitol completely suppresses the palladium extraction, and this combination is also the most efficient in hindering zirconium extraction. None of the masking agents have any notable effect on the cadmium extraction.

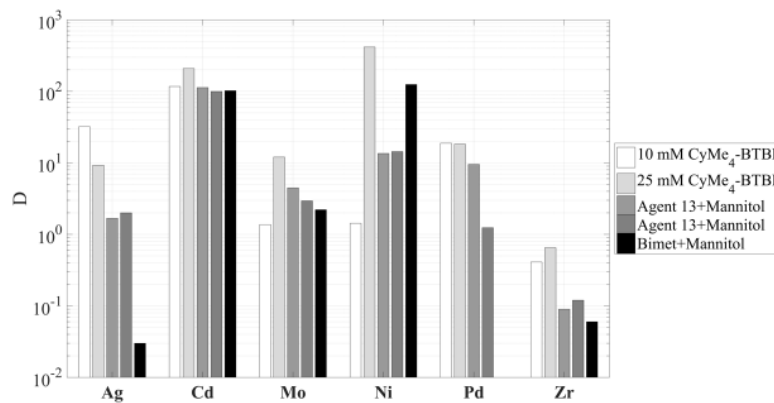


Figure 10. The distribution ratios of important fission products from a simulated PUREX raffinate. The extraction in the presence of masking agents were done with 25 mM CyMe<sub>4</sub>-BTBP.

Also the actinide extraction varies for the different systems. Not unexpectedly, the distribution ratio of all actinides except uranium is significantly increased in the system with higher CyMe<sub>4</sub>-BTBP. The addition of masking agents also have an effect on the distribution ratios. D(Am) is slightly decreased in the presence of agent 10 and agent 13, while an increase in D-value is seen for the bimetal system. Comparable trends are seen for D(Cm) and D(Eu). D(Eu) remains <1 in all systems.

Neptunium extraction appears to be slightly reduced by the addition of masking agents. For agent 10, the D-value is lower for the agent 10 system, compared to the pristine system with lowest CyMe<sub>4</sub>-BTBP concentration (10 mM). The same is seen for the uranium D-values, where it is clear that agent 10 also complexes uranium in the aqueous phase and thus preventing its extraction by the organic solvent. The other masking agents, agent 13 and bimetal, also significantly reduced D(U) compared to the pristine systems. This is surprising as earlier studies have shown that neither bimetal or mannitol reduces the uranium extraction, nor the extraction of any of the other actinides<sup>5</sup>. Further studies are therefore needed to understand this system behaviour. A slight reduction in D(Pu) is also seen, but the D-values are preserved at >10 and so it is of little concern.

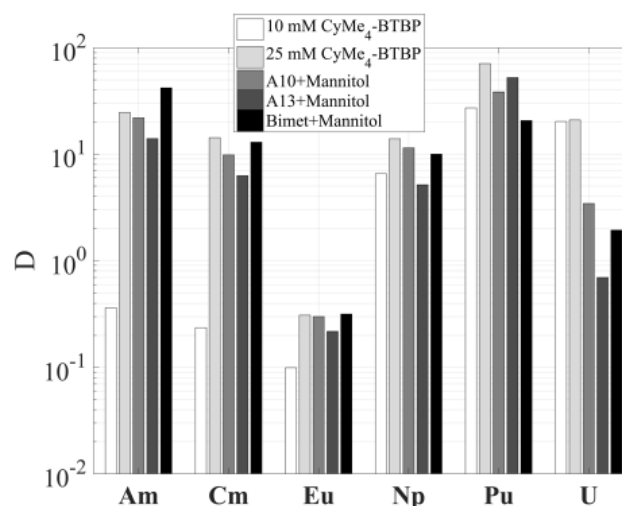
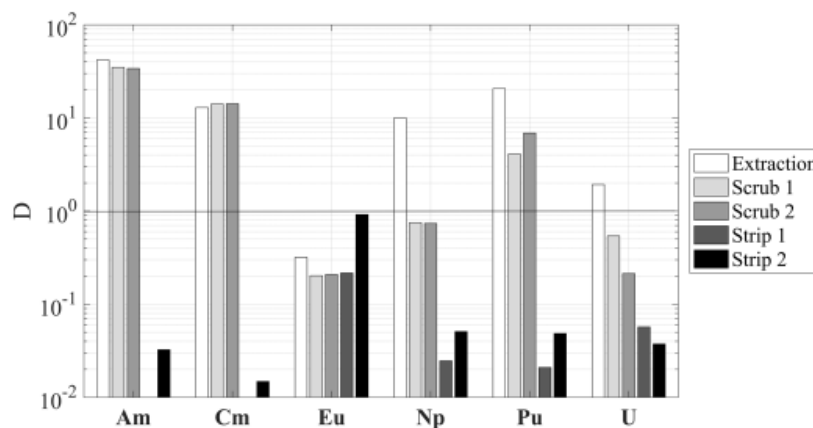


Figure 11. The distribution ratios of the actinides and europium resulting from increasing the ligand concentration and adding masking agents from a simulated PUREX raffinate.

Batch process flow diagrams were optimised as preparation for centrifugal contactor tests. The optimisations were based on the results reported earlier in WP 6 and earlier work. The results of the final batch flow sheet test can be seen in Figure 12 and Table 1. Each stage was allowed to reach equilibrium. It is clear that the combination of increased ligand concentration and addition of masking agents is sufficient to ensure good actinide/lanthanide separation. D-values for the extraction stage were in the range of those seen for the tests on simulated PUREX raffinate. The scrubbing steps (0.5M HNO<sub>3</sub>) however, back-extracts neptunium which is unwanted, with D-values <1. This could be due to the already low extractability of the Np(V) oxidation state, which in this HYPAR is reported to decrease with decreasing acid concentrations. This has also been found in other extraction systems<sup>6</sup>. Using 0.5 M glycolic acid as a stripping agent proved successful in back-extracting all actinides from the organic phase.

Flowsheet calculations were performed, and it was found that only 3 ideal extraction stages, 3 ideal scrubbing stages and 2 ideal stripping stage are required for a 99.9% overall recovery of americium. This gives less than 0.01% of americium loss in the scrubbing stages. For the same amount of stages, an overall recovery of 99% for curium and 94% for plutonium, while only a 61% and 40% recovery is achieved for neptunium and uranium however.



**Figure 12. The distribution ratios of the actinides and europium for the optimised batch flow sheet.**

The extraction and back-extraction of the most extracted fission products show promising results. Although cadmium, copper and nickel have high distribution ratios in the extraction stage and they remain in the organic phase during the scrubbing stages, they also remain in the organic phase during the stripping stages, ensuring a high purity actinide stream. Silver is not extracted to any significant degree and is also scrubbed in the scrubbing stages. This also applies to molybdenum: it is efficiently removed in the scrubbing stages.

**Table 1. The distribution ratios and pH for each process step in the batch flowsheet test.**

Process stage	pH	Ag	Cd	Cu	Mo	Ni	Pd	Zr
Extraction	-0.5	0.2	42	9.6	2.2	>100	0.0	0.0
Scrub 1	0.2	0.5	24	0.8	0.0	13	0.5	0.1
Scrub 2	0.3	0.5	16	1.3	0.3	>100	2.1	0.6
Strip 1	0.8	2.0	>100	9.0	5.9	94	>100	3.4
Strip 2	0.8	0.8	>100	1.9	>100	4.1	91	11

## 6.2 HETEROGENEOUS RECYCLING

### MAIN PROGRESSES

#### I-SANEX PTD DEMONSTRATION

Due to the COVID-19 pandemic, planned i-SANEX optimization studies using PyTri-Diol and a corresponding centrifugal contactor demonstration test had to be postponed. Nevertheless, chemical conditions and the planning were discussed with NNL and KIT. A new batch of PTD was synthesised at UNIPR and provided to JUELICH.

### CONCLUSIONS

Key technical highlights this semester include:

- ☑ Meeting MS9, EURO-GANEX trial complete and TRU nitrate product ready for conversion studies.
- ☑ Degree of Licentiate of Engineering defended and approved by a student at CHALMERS.
- ☑ 2 new journal publications on the CHALMEX process have been submitted and are under review.
- ☑ An important review article in T6.2 has been submitted to a journal by A. Geist, et al, entitled “An Overview of Solvent Extraction Processes Developed in Europe for Advanced Nuclear Fuel Recycling, Part 1 — Heterogeneous Recycling”

Manpower on the WP was similar (slight increase) from semester 5 but there are already impacts of the COVID- 19 pandemic with many partners’ laboratories shut down. Nevertheless, it remains likely that deliverables D6.2 and D6.3 will be delivered as planned (month 48).

**WP7****INTRODUCTION**

The objective of WP7 is to provide relevant dissolution and conversion processes linkable with the separation processes. When necessary, interfaces between dissolution/separation and separation/conversion are considered. For dissolution, the focus is put on the completion of data relevant for defining a dissolution model. The conversion issues of solutions from SX-process are the development of safe synthesis routes, the destruction of prejudicial organics from SX-process and characterization of synthesized MABB precursors. The workpackage is divided into 4 tasks: Task7.1 on dissolution, Task7.2 on destruction of organics, Task7.3 on development of safe synthesis routes and Task7.4 on characterization of MABB precursors

**MAIN RESULTS****TASK 7.1****MANPOWER**

Expected effort for the period 1.8 men.month

Actual effort spent during the period 1.8 men.month

**MAIN PROGRESSES**

The D7.1 report on dissolution model was written and validated

**ACTION PLAN**

No more work except writing of an article

**TASK 7.2****MANPOWER**

Expected effort for the period 1.5 men.month

Actual effort spent during the period 0.04 men.month

**MAIN PROGRESSES**

No significant progress this semester. Experimental programme has been planned and awaiting restart of laboratory operations

**DIFFICULTIES**

All laboratory work has been suspended due to COVID-19. Planned experiments to study the effect of complexants upon the precipitation of Pu oxalate have been postponed.

Abstract submitted to ATALANTE 2020. Conference has been cancelled due to COVID-19 impacts

A request has been made to delay D7.2 to month 48

---

### ACTION PLAN

Additional batch tests will be performed to evaluate the effect of acetic acid (AHA decomposition product) and PTD upon the precipitation of Pu oxalate.

---

### TASK 7.3

No significant progress obtained in this Task during this semester

---

### TASK 7.4 CHARACTERIZATIONS

No work in this Task during this semester

### CONCLUSION

During this semester, no progress was obtained in WP7 except achievement of D7.1.

**WP8****INTRODUCTION**

This WP addresses the industrialisation and scale up of some of the chemical projects studied in GENIORS. To develop processes towards industrialisation studies that consider the holistic impacts of the flowsheet are necessary. The tasks in this work package seek to assess and illustrate the holistic effects on the nuclear fuel cycle that occur from fundamental changes to the chemistry at the heart of its key processes. Appropriate technology deployment and consideration of potential issues and impediments to industrialisation will also be assessed.

**MAIN RESULTS****TASK 8.1 TO 8.3****TASK 8.4****MANPOWER**

None

**MAIN PROGRESSES**

Functional specifications for the Sim Plant model and user interface have been issued, providing clarity and direction to the ongoing development work. These documents clearly state what success will look like and provide a metric to which we can monitor our progress. In addition, guidelines have been established for process modellers working on the Sim Plant project such that all flowsheets and models developed are compatible with one-another.

The existing Excel-based Sim Plant HLW calculations have been converted into Gproms modelling software to enable better compatibility between current and future NNL models and flowsheets.

The Advanced PUREX and THORP PUREX reprocessing flowsheets have been constructed in gPROMS software to provide a baseline and comparison with the Euro-GANEX process.

Constructed an Excel-based front-end tool which links data output from FISPIN spent fuel inventory modelling code with the Sim Plant front end (The reprocessing flowsheet fuel feed). This removes a lot of manual work reducing time restrictions and data transfer errors.

The solid ILW, liquid effluent and Aerial effluent treatment routes on the Sellafield site have been researched and models have been constructed and combined with the existing HLW model.

Therefore, the Sim plant model is almost at a point where the entire waste route process can be modelled from a flowsheeting perspective. Efforts will be directed to constructing footprint and volume assessments from February 2020.

This was a knowledge capture exercise coordinated through the Sim Plant project team. Early career scientists and engineers were invited.

### ACTION PLAN

Capability to simulate a flowsheet from spent fuel to waste container. Further development of Sim Plant for plant footprint and plant sizing to begin (funded by UK leverage).

### TASK 8.5

### MANPOWER

1.5 pm has been reported.

### MAIN PROGRESSES

- Desk research has been performed.
- D8.3 has been analysed and scenarios have been revaluated.
- Interview questions have been prepared.
- Initial contribution from EDF and NNL have been acquired.

### DIFFICULTIES

- Decline in nuclear energy interest in the EU resulted in abandoning the fast reactor project, namely ASTRID by CEA. This adversely affect the implementation of scenarios that were developed for the transmutation of the most radiotoxic elements from spent fuel.
- Difficult to access to the interviewee from Orano which is a contributor for the report.

### ACTION PLAN

- Interviews will be taken place in the coming days.
- During next workshop, the results will be discussed.
- New interviewee and expert inputs will be needed. Thus, attendance to various GEN IV conferences and other related events can be targeted.

## CONCLUSIONS

Expert input is needed. The initial findings should be validated.

## WP9

### INTRODUCTION

Work Pack 9 aims to develop an emerging process towards industrialisation it is essential to understand from the outset what the safety implications of the process are and where efforts need to be focused to understand further the risks which need to be mitigated through flowsheet design and engineering. This work package aims to study these requirements for both normal and mal-operations across the fuel cycle from head end dissolution through to powder formation for fuel manufacture.

### MAIN RESULTS

#### TASK 9.2

#### MANPOWER

IRSN – 0.26pm

#### MAIN PROGRESSES

#### GANEX 2<sup>ND</sup> PART DENSITY LAW

In the second part of the GANEX process [5], uranium has been separated from plutonium. As illustrated in Figure 1, the process is fed with 10 g/L of plutonium in 5.9 mol/L of nitric acid and 0.055 mol/L of CDTA. In this step of the process, plutonium is separated from neptunium, americium and lanthanides.

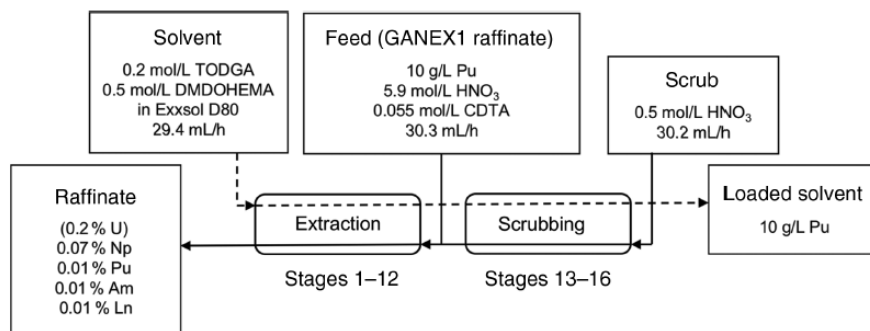


Figure 1: GANEX 2<sup>nd</sup> part process.

Once again, for the purpose of our study, nitric acid will be first neglected since it contributes to decrease the reactivity. The isotopic vector of plutonium is a vector traditionally used in criticality to bound plutonium media encountered in the nuclear fuel cycle. It is the following:

- $^{239}\text{Pu}$ : 71 wt%,
- $^{240}\text{Pu}$ : 17 wt%,
- $^{241}\text{Pu}$ : 11 wt%,
- $^{242}\text{Pu}$ : 1 wt%.

Room temperature (20 °C) is retained.

Uranium and CDTA will be neglected since their content is very low. Neglecting uranium contributes to an increase of reactivity since plutonium is more conservative than uranium in terms of criticality. The density of the solution is calculated using formula (3).

The density of the solvent-diluent is calculated using formula (4).

$$\rho_{\text{solution}} = C(\text{Pu}(\text{NO}_3)_4) + \rho_{\text{solvent-diluent}} \times \left(1 - \frac{C(\text{U})}{\rho(\text{U})} - \frac{C(\text{Pu})}{\rho(\text{Pu})}\right) \quad (3)$$

$$\rho_{\text{extractant-diluent}} = \left( C(\text{TODGA}) + C(\text{DMDOHEMA}) + \rho_{\text{diluent}} \times \left(1 - \frac{C(\text{TODGA})}{\rho(\text{TODGA})} - \frac{C(\text{DMDOHEMA})}{\rho(\text{DMDOHEMA})}\right) \right) \quad (4)$$

With  $\rho_{\text{diluent}}$  being the density of EXXSOL at 15 °C.

T is the temperature.

$\rho(\text{solvent} - \text{diluent})$  is the density of the solvent at 20 °C.

$C(\text{TODGA})$  is the concentration of TODGA in g/cm<sup>3</sup>.

$C(\text{DMDOHEMA})$  is the concentration of DMDOHEMA in g/cm<sup>3</sup>.

$\rho(\text{TODGA})$  is the density of TODGA at 20 °C in g/cm<sup>3</sup>.

$\rho(\text{DMDOHEMA})$  is the density of DMDOHEMA at 20 °C in g/cm<sup>3</sup>.

## COLLECTION OF DATA

The majority of extractants/diluents densities were found in the literature or were provided by participants to the GENIORS project. All these data are gathered in Table 1.

Table 1: Main characteristics of solvents and behaviour versus temperature

Extractant/diluent	Reference concentration of extractant in diluent (mol/L)	Density in g/cm <sup>3</sup>	Chemical formula	Behaviour versus temperature	Reference
TPH		0.7551 (25 °C)	C <sub>12</sub> H <sub>26</sub>	0.7551 × (1 - 0.0009826 × (T-25))	Data from Christian Sorel (see Table 2The data are gathered in Table 2. Table 2)

<b>DEHIBA</b>	1.151	0.8638 (25 °C)		$C_{20}H_{41}NO$	$-0.00066 \times (T-25) + 0.8638$	PhD works [6]
<b>EXXSOL</b>		0.798 (15 °C)	0.684	n-heptane - $C_7H_{16}$	$-0.00068 \times (T-15) + \rho (15\text{ °C})$	Analogy with TODGA/DMDOHEMA behaviour)
			0.7786	cyclohexane $C_6H_{12}$		
			0.6594	n-hexane $C_6H_{14}$		
			0.77	methylcyclohexane $C_7H_{14}$		
<b>TODGA</b>	0.2	0.9054 (25 °C)		$C_{36}H_{72}N_2O_3$	$-0.00066 \times T + 0.9219$	Data from Justine Cambe-Issaadi, Anne Lélías (CEA) (See Table 3)
<b>DMDOHEMA</b>	0.5	0.914 (25 °C)		$C_{29}H_{58}N_2O_3$	$-0.00068 \times T + 0.931$	

Density of organic solutions involved in the GANEX 1<sup>st</sup> cycle have been measured in order to estimate flowrates variations with composition and temperature in our simulation code PAREX. In addition, the knowledge of the organic density is useful to convert organic concentration from the molarity scale (mol/L) to the molality scale (mol/kg) which is retained for the modelling of extraction and complexation equilibria in our code. All the density data have been measured with an Anton-Paar density meter.

Density of TPH has been measured on the temperature range 20-60°C. The data are gathered in Table 2.

Table 2: Density of DEHIBA solution versus temperature.

[DEHiBA] (mol/l)	T (°C)	$\rho_{exp}$ (g/ml)
1.49	25	0.8137
1.49	35	0.8065
1.49	45	0.7991
0.99	25	0.7949
0.99	35	0.7877
0.99	45	0.7805

From these data, it is possible to establish the behavior of the density versus temperature as it is given in Table 1.

Regarding the GANEX 2<sup>nd</sup> phase, acquisition of densities of the pure TODGA and DMDOHEMA was performed from 15 to 55°C, using a SVM 3000 densimeter (ANTON PAAR). Justine Cambe-Issaadi and Anne Lélías (CEA) provided the data to IRSN. Each data is the mean value of two measurements and is reported in Table 3.

From these data, it is possible to establish the behavior of the density versus temperature as it is given in Table 3.

Table 3: Measurement of TODGA and DMDOHEMA densities versus temperature.

T (°C)	Density (g/cm <sup>3</sup> ) ± 0.0002 g/cm <sup>3</sup>	
	TODGA	DMDOHEMA
55	0.8857	0.8936
45	0.8923	0.9005
35	0.8988	0.9072
25	0.9053	0.914
15	0.9120	0.9208

## COMPARISON OF CRITICALITY STANDARDS

In order to compare the reactivity worth induced by the change of solvent/diluent, a Monte Carlo calculation using the MORET 5.D.1 code [9] is performed using the critical dimensions determined for the water solvent/moderator with the compositions obtained for an organic solvent/diluent. It is a good way to traduce in terms of reactivity worth the penalizing effect of the solvent/diluent. The results are reported for the three geometries in Figure 2 for the first step of the EURO-GANEX process.

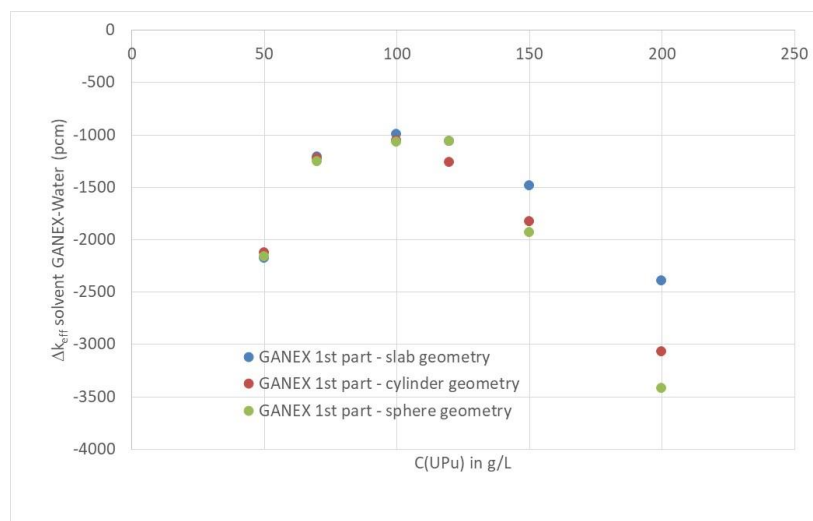


Figure 2:  $k_{eff}$  discrepancy versus solvent/diluent nature – GANEX 1<sup>st</sup> phase

## TASK 9.3

### MANPOWER

ULanc – 6pm

### MAIN PROGRESS

Continued corrosion assessments of a further inventory permutation have been carried out this period, specifically hydrazine on its own and in the presence/absence of Trans-1,2-diaminocyclohexane-N,N,N',N'-tetraacetic acid (CDTA). SS316L and 18/10 NAG (Nitric Acid Grade) electrodes have been used in the investigation of the corrosive behaviour of 0.2 mol dm<sup>-3</sup> hydrazine in 1.5 mol dm<sup>-3</sup> nitric acid. The 18/10 NAG steel is a specialist grade of nitric acid resistant stainless steel plate used in the Thermal Oxide Reprocessing Plant (THORP) at Sellafield, Cumbria, UK.

In addition to its reductant properties, hydrazine is known to be a corrosion inhibitor. From the data presented below, adsorption of a hydrazine film at anodic pore sites is thought to cause a blocking of such sites and an overall reduction in corrosive pitting attack through pitting. The additional of hydrazine is found here to cause two important observable effects:

- (1) The corrosion potential ( $E_{corr}$ ) in the presence of hydrazine is shifted  $\sim 30$  mV more positive resulting in movement of the anodic arm of the tafel plot towards the region of primary passivation in the log(current) vs applied potential plot.
- (2) Currents within the transpassive range are significantly reduced, suggesting a stabilisation of a secondary passivation layer in the presence of hydrazine and This latter effect is observed in both the N<sub>2</sub> and air sparged solutions, with hydrazine having an almost identical inhibition effect in the transpassive region.

The corrosion inhibition of steel wire electrodes in the presence of CDTA was described in the last reporting period. Here, the mechanism has been investigated further using the high surface area electrodes detailed above, providing data for systems closer to realistic conditions and with observable surface morphologies. While LSV/Tafel curves for hydrazine-nitric acid systems shows the stabilisation of a secondary passive layer in the region of transpassive dissolution (where intergranular corrosion may occur), such a stabilisation is not observed with CDTA. However, transpassive currents are still reduced at transpassive potentials, suggesting that the inhibitive action of CDTA is more akin to restricting solution access to the electrode surface. Again this corrosion inhibition action is exclusive of atmospheric condition.

Finally, when CDTA is present in combination with hydrazine and nitric acid transpassive currents are lowered further than those observed independently of the addition of each

agent. Thus, it would appear that both hydrazine and CDTA can act in combination to inhibit transpassive corrosion if both are present in solution.

In addition to the above none radioactive experiments, preliminary longer term corrosion studies under realistic gamma irradiation conditions have been carried out on SS304L steel foils in solutions of nitric acid with and without the presence of CDTA. Tentative SEM results suggest that CDTA, as in non-gamma irradiated experiments, provides some protection to intergranular attack under nitric acid/gamma irradiation.

See ULanc HYPAR for full details.

**WP10**

The objective of WP10 is to integrate the work done in GENIORS in a more global approach by creating synergies with other European and international initiatives and by involving the stakeholders. This is done via Clustering Events and Stakeholders Events.

**MAIN RESULTS****TASK 10.1 CLUSTERING EVENTS****MANPOWER**

Globally on track.

**MAIN PROGRESS****D10.3**

Clustering Event “ATALANTE 2020” was defined and to be organized in June 2020. However, due to Covid-19 pandemic, the conference was cancelled.

**D10.4**

Clustering Event “Partitioning meets Conditioning” was defined and to be organized in October/November 2020. However, due to Covid-19 pandemic, the event was cancelled.

**DIFFICULTIES**

D10.2 – Clustering Event “INSPIRE summer school” – still to be written.

D10.3 – Clustering Event “ATALANTE 2020” – cancelled due to Covid-19 pandemic.

D10.4 – Clustering Event “Partitioning meets Conditioning” – cancelled due to Covid-19 pandemic.

**ACTION PLAN**

Write deliverable D10.2 (CEA).

Define new date & venue for D10.3 and D10.4 or define alternative (SCK CEN and CEA).

**TASK 10.2 STAKEHOLDERS EVENTS**

No progress this period.

**DIFFICULTIES**

D10.5 – Stakeholders Event “Partitioning meets Transmutation” – still to be written.

---

### ACTION PLAN

Write deliverable D10.5 (CEA).

### CONCLUSIONS

Summary status of organizing Clustering/Stakeholders Events:

2 Clustering Events (D10.1 – “Partitioning meets Transmutation” and D10.2 – “INSPIRE summer school”) and 1 Stakeholders Event (D10.5 – “Partitioning meets Transmutation”) have been organized.

2 Clustering Events and 1 Stakeholders Event are still to be organized. Clustering Events 3 (related to D10.3) and 4 (related to D10.4) need to be rescheduled or an alternative needs to be defined. Stakeholders Event 2 (related to D10.6) is foreseen at the end of the project.

**WP12****INTRODUCTION**

This work package covers Training and Education and Knowledge Management. Work on the tasks has largely proceeded as planned.

**MAIN RESULTS****TASK 421****MANPOWER**

ULEEDS: 0.1pm

**MAIN PROGRESSES**

To date there have been 6 awards - four secondments and two travel bursaries - with a total value of €10,542

**ACTION PLAN**

Continue to encourage applications to the fund.

**TASK 422**

This task is complete.

**TASK 423****MANPOWER**

ULEEDS: 0.10 pm

**MAIN PROGRESSES**

The course outline has been created and the script/content of the packages is being developed with Leeds Digital Education Service.

**ACTION PLAN**

Continue to develop the course script/content.

Produce draft package on PUREX by 30th May 2020. Although this date will not be met due to restricted access to ULEEDS Digital Education Service